$3 \times 10^5$, or $5 \times 10^5$/200 μL) 2 hours later on day 0. B16 melanoma cells were prepared as previously described.[11,16] Some mice were primed 2.5 days earlier with OCH or α-GalCer. Some mice were administered with 300 μg of isotype-matched control Ig or anti-NKG2 mAb intraperitoneally 2 days before the last α-GalCer injection. On day 14, the number of tumor colonies on the lungs was counted under a dissecting microscope (Olympus, Tokyo, Japan).

### Statistical analysis

Data were analyzed by a 2-tailed Student *t* test. *P* values less than .05 were considered significant.

## Results

### Modulation of costimulatory and NK-cell receptors on iNKT cells upon priming with TCR ligands

We analyzed the modulation of TCR, inhibitory NK-cell receptors (CD94/NKG2 and Ly49A/C/I/G2), activating NK-cell receptors (NK1.1, NKG2D, and Ly49D), and a costimulatory receptor (CD28) on iNKT cells after in vivo priming with synthetic TCR ligands, α-GalCer or OCH. Amongst liver iNKT cells from B6 WT mice, approximately 50% expressed CD94/NKG2 and NKG2D, less than 10% expressed Ly49A/C/I/G2, less than 2% expressed Ly49D, and all constitutively expressed CD28 (Figure 1A). Staining with an NKG2A-specific mAb showed that CD94/NKG2 expressed on iNKT cells was mainly composed of NKG2A (data not shown) but not NKG2C or NKG2E, as previously reported.[22] Upon priming with α-GalCer or OCH, α-GalCer/CD1d tetramer$^+$ iNKT cells seemingly began to disappear within 6 hours (data not shown) and almost completely disappeared at 16 to 24 hours, as previously reported.[15-20] Consistent with recent reports,[18-20] intracellular staining with anti-Vβ2/7/8 mAbs, detecting the predominant TCR β-chains expressed by iNKT cells, clearly showed the presence of liver iNKT cells expressing intracellular TCR at 24 hours after α-GalCer or OCH priming. NK-cell receptors and CD28 were also internalized, although some retention of cell surface CD28 was still detected (Figure 1A). Although staining intensity was relatively weak, intracellular staining with α-GalCer–loaded recombinant soluble dimeric mouse CD1d:Ig also demonstrated the internalized α-GalCer/CD1d–specific TCR coexpressed with intracellular NK1.1 one day after α-GalCer (Figure 1B) or OCH injection (data not shown). Similar results were obtained with spleen MNCs after in vivo priming and with liver MNCs after in vitro priming (data not shown).

After 2 to 3 days, the primed iNKT cells re-expressed TCR and CD28 on their surface. By contrast, a reduced level of surface NK-cell receptors (NK1.1, CD94/NKG2, Ly49, and NKG2D) was maintained for at least 3 to 4 days. After 5 to 7 days, some iNKT cells still expressed a low level of surface NK1.1, but another iNKT-cell population expressed relatively higher levels of NK1.1 compared with naive iNKT cells. After activation, the proportions of CD94/NKG2-, Ly49-, or NKG2D-expressing iNKT cells increased, and the expression levels of CD94/NKG2 and Ly49 were relatively higher than those found on naive iNKT cells. Again, CD94/NKG2 on these iNKT cells was mainly composed of NKG2A as estimated by staining with NKG2A-specific mAb. Consistent with previous reports,[7,9,18-20] TCR ligand priming induced iNKT-cell expansion, although the expansion level was reduced following OCH priming (1.5-3 fold) compared with α-GalCer priming (5-8 fold) (data not shown). Similar results were obtained with spleen MNCs after in vivo priming and with liver MNCs after in vitro priming (data not shown).

Consistent with a previous report that OCH selectively induced T-helper 2 (Th2) cytokine production by iNKT cells,[6] a minor but significant serum IL-4 elevation was observed 3 to 5 hours after priming with OCH, but serum IFN-γ was not detected (Figure 2A). Moreover, we observed a similar modulation of iNKT-cell surface

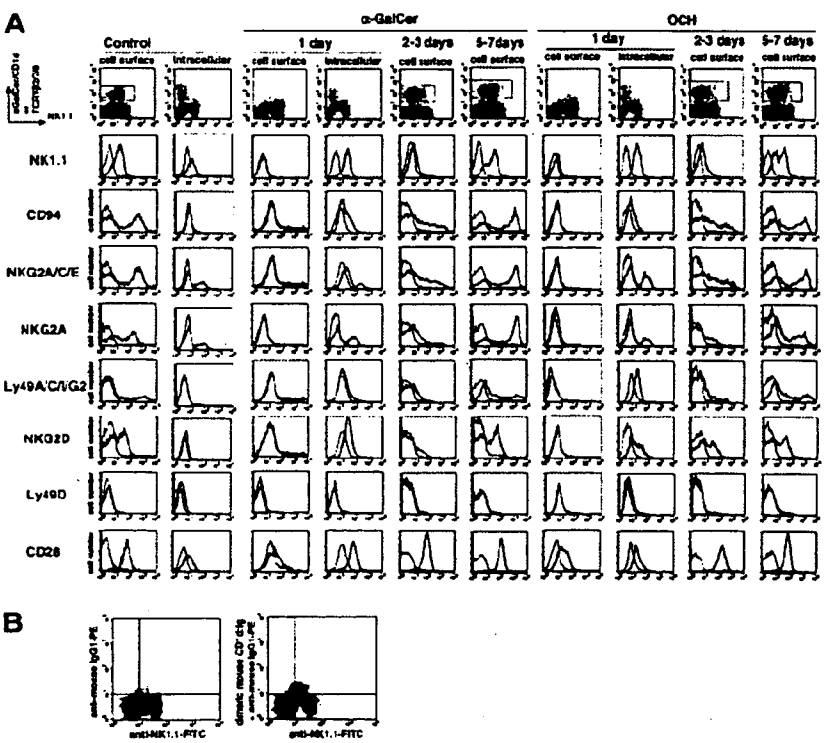


**Figure 1. Modulation of NK1.1, CD94/NKG2, Ly49, NKG2D, and CD28 on α-GalCer– or OCH-activated liver iNKT cells.** (A) Cell surface expression of the indicated molecules was analyzed on electronically gated α-GalCer/CD1d$^+$ iNKT cells on the indicated days after intraperitoneal injection of α-GalCer or OCH. One day after α-GalCer or OCH injection, both cell surface and intracellular expression of the indicated molecules were analyzed in electronically gated intracellular Vβ2/7/8$^+$ iNKT cells. The analysis gates are indicated by the gray line in dot plot panels. Bold lines indicate the staining with the respective mAb, and the thin lines indicate the staining with isotype-matched control Ig. Similar results were obtained from 3 independent experiments. (B) Existence of a cell population expressing intracellular α-GalCer/CD1d–specific TCR 1 day after α-GalCer injection. Liver MNCs were intracellularly stained with α-GalCer–loaded recombinant soluble dimeric mouse CD1d:Ig and PE-conjugated anti–mouse IgG1 mAb, or PE-conjugated anti–mouse IgG1 mAb together with FITC-conjugated anti-NK1.1 mAb, 1 day after α-GalCer injection. Quadrant gates were set by staining with FITC-conjugated isotype-matched control and PE-conjugated anti–mouse IgG1 mAb.

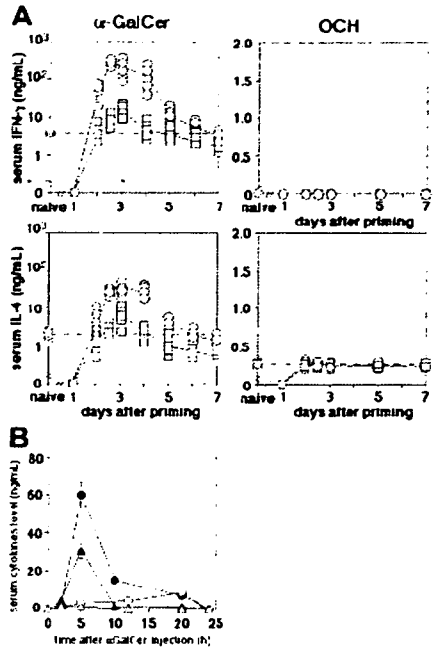


**Figure 2. Augmented serum IFN-γ and IL-4 following α-GalCer treatment in OCH-primed mice.** (A) Mice were primed with intraperitoneal injection of α-GalCer (□) or OCH (○) and then boosted with α-GalCer or OCH on the indicated day. Serum samples were obtained from 3 to 10 mice in each group 5 hours after the boost or the priming. Serum IFN-γ and IL-4 levels of primed naive mice were indicated on the y-axis (○), and the dotted horizontal line in each panel shows the mean level of the primary response. Serum IFN-γ or IL-4 in the vehicle-injected mice were not detectable (data not shown). (B) Kinetics of serum IFN-γ (circles) and IL-4 (triangles) levels following α-GalCer boost of vehicle-primed (open symbols) or OCH-primed (closed symbols) mice on day 2.5. Data are represented as the mean ± SD of 5 mice in each group. Similar results were obtained from 3 independent experiments.

receptors by α-GalCer or OCH priming in IFN-γ$^{-/-}$ mice or in anti–IFN-γ mAb– and/or anti–IL-4 mAb–treated WT mice (data not shown). Taken together, these results indicated that priming of iNKT cells with TCR ligands resulted in a dramatic modulation of not only TCR and NK1.1 but also CD28 and inhibitory or activating NK-cell receptors on their surface, and this modulation was independent of IFN-γ or IL-4 production.

### Augmented recall responses of OCH-primed iNKT cells to α-GalCer in vivo

Since the modulation of surface receptors on iNKT cells by Ag priming might modify iNKT-cell responses to subsequent Ag challenge, we next examined the responses of α-GalCer– or OCH-primed mice to secondary α-GalCer or OCH administration. We measured serum IFN-γ and IL-4 5 hours after α-GalCer or OCH injection to avoid the contribution of NK cells, since it has been previously reported that NK cells are activated after iNKT-cell activation and contribute significantly to IFN-γ production within 12 hours after α-GalCer injection.[16,31] Of interest, serum IFN-γ and IL-4 levels were dramatically increased (10-30 fold) by secondary α-GalCer injection 2 to 4 days after OCH priming compared with primary α-GalCer injection (Figure 2A). By contrast, serum IFN-γ and IL-4 levels were only slightly increased by secondary α-GalCer injection in α-GalCer–primed mice compared with primary α-GalCer injection (Figure 2A). Very little serum IFN-γ and IL-4 were detected in mice injected with α-GalCer 1 day after α-GalCer or OCH priming, possibly due to the initial internalization of TCR in iNKT cells. OCH administration after α-GalCer or OCH priming did not augment serum IL-4 levels compared with primary administration of OCH, and serum IFN-γ was never detected (Figure 2A). We also examined the kinetics of serum IFN-γ and IL-4 induction by α-GalCer injection 2.5 days after OCH priming. Both IFN-γ and IL-4 levels were dramatically increased by the OCH priming and peaked at 5 hours after secondary α-GalCer injection (Figure 2B).

We next examined the α-GalCer–induced cytotoxic activity and antitumor effect in α-GalCer– or OCH-primed mice. OCH priming markedly augmented the α-GalCer–induced cytotoxic activities of liver and spleen MNCs against either NK-cell–sensitive YAC-1 or NK-cell–resistant P815 target cells compared with priming with the vehicle (Figure 3A). However, the iNKT-cell proportions in MNCs were similar among the groups when the mice were boosted by secondary α-GalCer injection (Table 1). In contrast, α-GalCer priming did not significantly augment the secondary α-GalCer–induced cytotoxicity (Figure 3A). Moreover, α-GalCer administration 2.5 days after OCH priming markedly augmented the antimetastatic effect against B16 melanoma compared with other prime/boost regimens (eg, α-GalCer/α-GalCer; Figure 3B). These results indicated that iNKT cells were hyperresponsive to secondary α-GalCer stimulation 2 to 3 days after OCH priming in vivo, resulting in a dramatic augmentation of effector functions, including IFN-γ and IL-4 production, cytotoxicity, and antitumor effect.

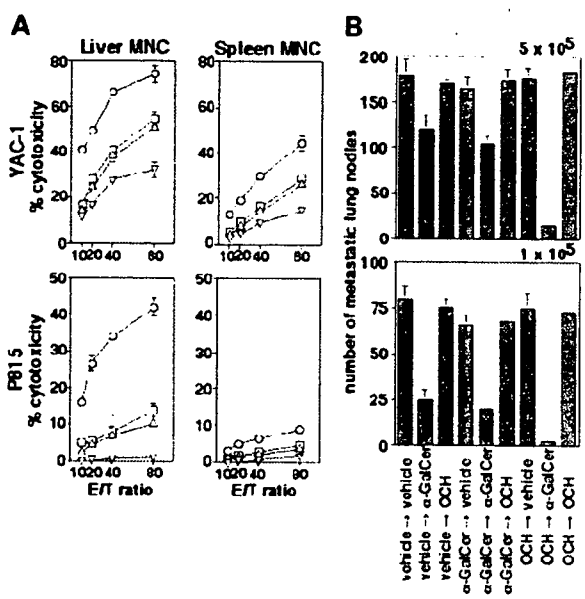


**Figure 3. Induction of cytotoxic activity and antimetastatic effect by priming and boosting with α-GalCer and OCH.** (A) Cytotoxic activity of liver and spleen MNCs was tested against NK-cell–sensitive YAC-1 cells or NK-cell–resistant P815 cells 24 hours after α-GalCer injection into mice primed 2.5 days earlier with vehicle (△), αGalCer (□), or OCH (○). Control mice were primed and boosted with vehicle (▽). Proportion of iNKT cells (%) in respective MNC populations at the time of boosting injection is indicated in Table 1. Data are represented as the mean ± SD of triplicate samples. Similar results were obtained from 3 independent experiments. E/T indicates effector-to-target ratio. (B) Antimetastatic effect. Mice were primed and boosted with α-GalCer, OCH, or vehicle on days −3 and 0 as indicated. Then, the indicated number of B16 melanoma cells were intravenously inoculated into the mice 2 hours after the boost. On day 14, the number of tumor metastatic colonies in the lungs was counted. Data are represented as the mean ± SD of 5 mice in each group. Similar results were obtained from 3 independent experiments.

**Table 1. Proportion of iNKT cells in respective MNC populations at the time of boosting injection**

| | Liver MNCs, % | Spleen MNCs, % |
|---|---|---|
| Vehicle primed | 22.7 ± 4.4 | 1.7 ± 0.8 |
| α-GalCer primed | 24.5 ± 3.4 | 3.3 ± 1.8 |
| OCH primed | 23.6 ± 5.1 | 2.5 ± 1.5 |

### Suppression of α-GalCer–induced iNKT-cell activation by Qa-1$^b$ and CD94/NKG2A interaction

To evaluate the priming effects more precisely, spleen MNCs were periodically isolated from naive, α-GalCer–primed, or OCH-primed mice and then stimulated with α-GalCer or OCH in vitro (Figure 4A). At 24 hours after the in vitro stimulation with α-GalCer or OCH, spleen MNCs from naive mice did not produce either IFN-γ or IL-4 at detectable levels, but by contrast spleen MNCs from α-GalCer– or OCH-primed mice produced substantial amounts of IFN-γ and IL-4 (Figure 4A). Maximal cytokine secretion was obtained from spleen MNCs isolated 2.5 days after priming. Consistent with the in vivo data (Figure 2), OCH-primed spleen MNCs secreted greater amounts of cytokines compared with α-GalCer–primed spleen MNCs. At 48 to 72 hours after the in vitro stimulation, naive splenic MNCs produced substantial amounts of IFN-γ and IL-4 in response to α-GalCer, but the OCH-primed MNCs still produced increased levels of both IFN-γ and IL-4 in response to α-GalCer restimulation compared with naive or α-GalCer–primed MNCs (data not shown). These results indicated that OCH priming sensitized iNKT cells to secondary α-GalCer stimulation more effectively than α-GalCer priming.

We next explored the mechanism by which OCH or α-GalCer priming sensitized iNKT cells to α-GalCer restimulation. We first examined whether the CD94/NKG2 inhibitory receptor might regulate the hyperresponsiveness of iNKT cells, since CD94/NKG2 was down-modulated on the sensitized iNKT cells 2 to 3 days after α-GalCer or OCH priming (Figure 1). Blockade of the CD94/NKG2 and Qa-1$^b$ interaction by Fab fragments of anti-NKG2 mAb or anti–Qa-1$^b$ mAb markedly enhanced IFN-γ and IL-4 production by α-GalCer–primed MNCs in response to restimulation in vitro with α-GalCer (Figure 4B). Albeit to a lesser extent, IFN-γ and IL-4 production by OCH-primed or naive MNCs was also significantly enhanced by the blockade of Qa-1$^b$ or CD94/NKG2. Notably, while α-GalCer–primed MNCs produced lower levels of IFN-γ and IL-4 than OCH-primed MNCs in response to α-GalCer restimulation in vivo, this difference was abrogated by the blockade of Qa-1$^b$ or CD94/NKG2. The contribution of activating CD94/NKG2C/E NK-cell receptors may be negligible, since blockade of the Qa-1$^b$–CD94/NKG2 interaction did not inhibit cytokine production by α-GalCer–activated iNKT cells in all cocultures, even if anti-NKG2 mAb or anti–Qa-1$^b$ mAb inhibited the function of activating CD94/NKG2C/E. Blockade of the CD80/CD86 interaction with CD28 abolished the cytokine production by naive or primed MNCs, irrespective of Qa-1$^b$ or CD94/NKG2 blockade. These results indicated that the Qa-1$^b$ and CD94/NKG2 interaction suppressed the TCR- and CD28-mediated activation of iNKT cells by α-GalCer, especially when the iNKT cells had first been primed with α-GalCer.

We also examined the impact of OCH or α-GalCer priming on antigen-presenting cells (APCs) by coculturing of purified iNKT cells and purified splenic DCs separately isolated 2.5 days after priming with α-GalCer, OCH, or vehicle (Figure 4C). Neither IFN-γ nor IL-4 was detected when iNKT cells were cocultured with any DCs in the absence of α-GalCer (data not shown). Notably, α-GalCer–primed DCs induced significantly lower levels of IFN-γ and IL-4 production by vehicle-primed iNKT cells compared with vehicle- or OCH-primed DCs. Of importance, this difference was abrogated by the blockade of CD94/NKG2. Moreover, OCH-primed iNKT cells produced significantly higher levels of IFN-γ and IL-4 compared with vehicle- or α-GalCer–primed iNKT cells. Again, the difference of cytokine production between OCH-primed and α-GalCer–primed iNKT cells was abrogated by CD94/NKG2 blockade. Significantly higher levels of IFN-γ and IL-4 were attained by both types of primed iNKT cells compared with vehicle-primed iNKT cells. A similar level (approximately 200 pg/mL) of IL-12 p40 was detected in the supernatants of all

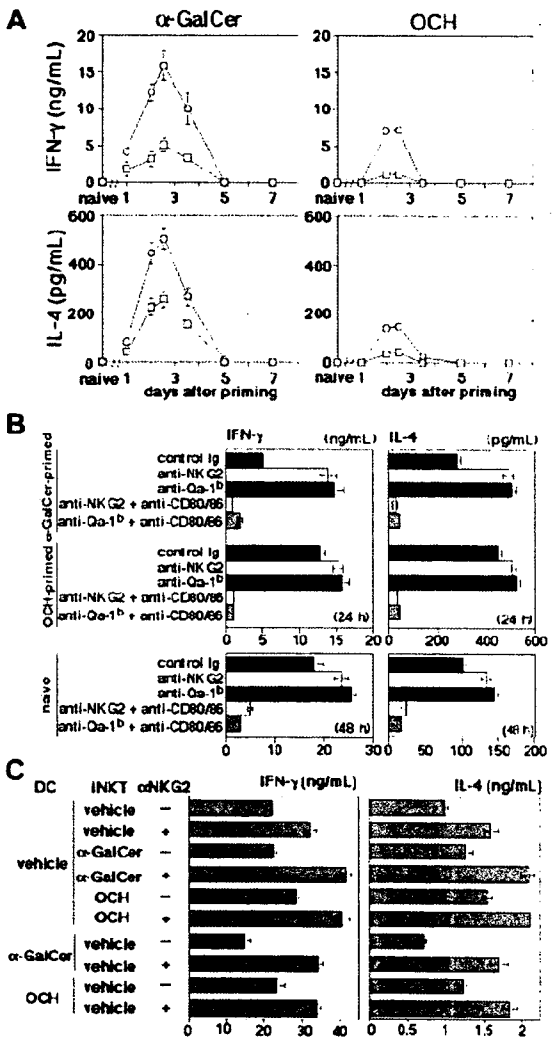


**Figure 4. NKG2 and CD28 regulate activation of naive or primed iNKT cells by α-GalCer.** (A) Mice were primed with intraperitoneal injection of α-GalCer (□) or OCH (○). Splenic MNCs were prepared on the indicated days after priming and stimulated with α-GalCer or OCH in vitro for 24 hours. Data are represented as the mean ± SD of triplicate wells. Similar results were obtained from 3 independent experiments. (B) Mice were primed with intraperitoneal injection of α-GalCer, OCH, or vehicle on day −2.5. Then, splenic MNCs were prepared on day 0 and stimulated with α-GalCer in vitro for 24 or 48 hours in the presence or absence of the indicated mAbs. Data are represented as the mean ± SD of triplicate wells. Similar results were obtained from 3 independent experiments. (C) Liver iNKT cells and splenic DCs were isolated from naive mice or primed with α-GalCer or OCH 2.5 days before and then cocultured with α-GalCer for 48 hours in the presence or absence of anti-NKG2 mAb. Data are represented as the mean ± SD of triplicate wells. Similar results were obtained from 2 independent experiments.

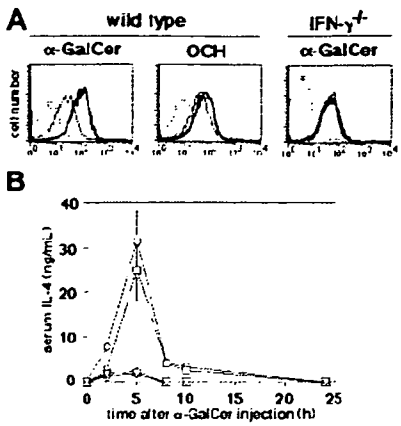


Figure 5. IFN-γ–induced Qa-1$^b$ inhibits reactivation of α-GalCer–primed iNKT cells by α-GalCer. (A) Qa-1$^b$ expression on splenic MNCs isolated from WT and IFN-γ$^{-/-}$ mice was analyzed 2.5 days after intraperitoneal administration of α-GalCer or OCH. Thin lines indicate the staining of MNCs from vehicle-treated mice with anti–Qa-1$^b$ mAb; bold lines, the staining of MNCs from α-GalCer– or OCH-treated mice with anti–Qa-1$^b$ mAb; and dotted lines, the staining with isotype-matched control Ig. Similar results were obtained from 3 independent experiments. (B) Kinetics of serum IL-4 induction after α-GalCer injection into vehicle-primed wild-type mice (▽), vehicle-primed IFN-γ$^{-/-}$ mice (△), α-GalCer–primed IFN-γ$^{-/-}$ mice (□), or OCH-primed IFN-γ$^{-/-}$ mice (○). Priming was performed 2.5 days before. Serum IL-4 was not detectable in the vehicle-injected mice (data not shown). Data are represented as the mean ± SD of 5 mice in each group. Similar results were obtained from 3 independent experiments.

cocultures (data not shown), which suggested that DC function was not impaired by α-GalCer or OCH priming. These results suggested that the recall responses of iNKT cells in α-GalCer–primed mice were more strictly regulated by Qa-1$^b$ and CD94/NKG2-mediated suppression than in naive or OCH-primed mice. Consistent with this notion, Qa-1$^b$ expression on splenic MNCs was markedly up-regulated in α-GalCer–primed mice compared with naive or OCH-primed mice (Figure 5A).

### IFN-γ–induced Qa-1$^b$ expression negatively regulates recall NKT-cell responses in vivo

Although iNKT cells primed with α-GalCer strongly up-regulated the Qa-1$^b$ expression on splenic MNCs, those primed with OCH did so only weakly (Figure 5A). Notably, the α-GalCer–induced Qa-1$^b$ up-regulation was not observed in IFN-γ$^{-/-}$ mice (Figure 5A). Moreover, α-GalCer priming increased the secondary α-GalCer–induced serum IL-4 to a level comparable with that induced by OCH priming in IFN-γ$^{-/-}$ mice (Figure 5B). These results indicated that IFN-γ induced by α-GalCer priming was responsible for Qa-1$^b$ up-regulation, which in turn resulted in CD94/NKG2-mediated suppression of recall iNKT-cell response in α-GalCer–primed mice.

We finally evaluated whether the blockade of CD94/NKG2 could augment the α-GalCer–induced iNKT-cell function in α-GalCer–primed mice. The in vivo treatment with anti-NKG2 mAb alone did not induce cytokine production or cytotoxicity and did not deplete NK cells or iNKT cells (data not shown). The CD94/NKG2 blockade dramatically increased α-GalCer–induced serum IFN-γ and IL-4 levels, particularly in α-GalCer–primed mice (Figure 6A). It was notable that high levels of serum IFN-γ and IL-4 were inducible 10 days after α-GalCer priming if CD94/NKG2 was blocked at the time of boosting. Moreover, the CD94/NKG2 blockade also significantly augmented the α-GalCer–induced cytotoxicity of liver and spleen MNCs and the antimetastatic effect of treatment, particularly in α-GalCer–primed mice (Figure 6B-C). Even if anti-NKG2 mAb possibly inhibited the function of activating CD94/NKG2C/E, the contribution of activating CD94/NKG2C/E NK-cell receptors may be negligible, since blockade of the Qa-1$^b$–CD94/NKG2 interaction did not inhibit

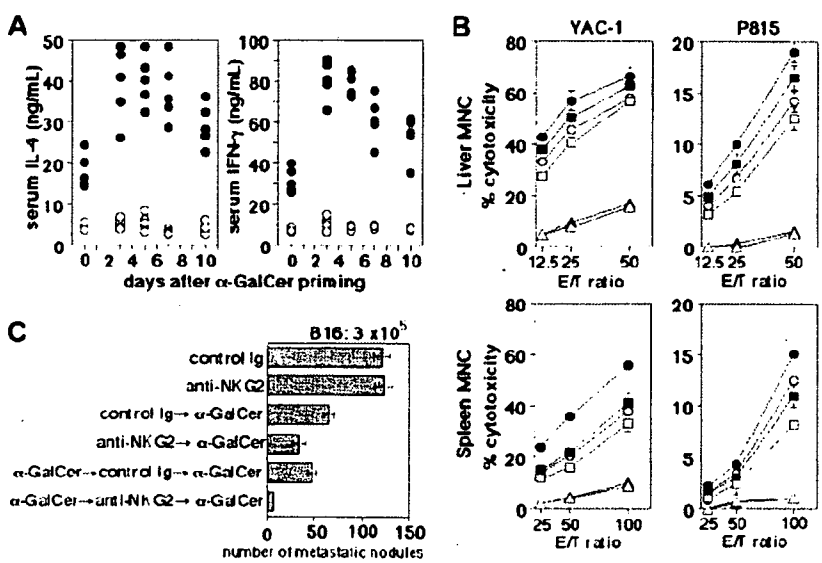


Figure 6. Blockade of NKG2 enhances activation of naive and α-GalCer–primed iNKT cells by α-GalCer in vivo. (A) Mice were primed with α-GalCer on day 0 and then boosted with α-GalCer on the indicated day. Anti-NKG2 mAb (●) or control Ig (○) was administered 2 days before the boost. Serum samples were obtained 5 hours after the boost. The mice indicated on day 0 were treated once with α-GalCer injection on day 0. (B) Cytotoxic activity of liver and spleen MNCs was tested against NK-sensitive YAC-1 cells and NK-resistant P815 cells 24 hours after the last α-GalCer injection. Mice were intraperitoneally injected with α-GalCer on day 0 (squares) or days −3 and 0 (circles), or injected with vehicle on days −3 and 0 (triangles), and intraperitoneally administered with anti-NKG2 mAb (closed symbols) or control Ig (open symbols) on day −2. Data are represented as the mean ± SD of triplicate samples. Similar results were obtained from 3 independent experiments. (C) Antimetastatic effect. Mice were intraperitoneally injected with α-GalCer on day 0 or days −3 and 0, and then intravenously inoculated with 3 × 10$^5$ B16 melanoma cells 2 hours later. Anti-NKG2 mAb or control Ig was intraperitoneally administered on day −2. On day 14, the number of tumor colonies in the lungs was counted under a dissecting microscope. Data are represented as the mean ± SD of 5 to 8 mice in each group. Similar results were obtained from 3 independent experiments.

cytokine production, cytotoxic activity, or the antimetastatic effect caused by the α-GalCer injection. These results indicated that the iNKT-cell activation by α-GalCer was limited by CD94/NKG2-mediated suppression and blockade of CD94/NKG2 could significantly improve the antitumor effect of a secondary α-GalCer treatment.

## Discussion

In this study, we have shown that activation of iNKT cells is critically regulated by CD94/NKG2. In addition to TCR and CD28, naive iNKT cells express activating (NK1.1, NKG2D, and Ly49D) or inhibitory (CD94/NKG2 and Ly49A/C/I/G2) NK-cell receptors. All of these cell surface receptors were rapidly down-modulated upon priming of iNKT cells with their TCR ligands (α-GalCer or OCH). Two to 3 days after the priming, iNKT cells re-expressed TCR and CD28 on their surface, but CD94/NKG2 and Ly49 remained down-modulated. This pattern of expression enabled the primed iNKT cells to produce a larger amount of cytokines upon secondary stimulation with α-GalCer. Of interest, OCH was superior to α-GalCer in priming iNKT cells for a secondary response to α-GalCer, resulting in a markedly enhanced antimetastatic effect. We found that IFN-γ induced by α-GalCer priming up-regulated Qa-1$^b$, which in turn suppressed the secondary iNKT-cell activation via CD94/NKG2. Thus, the blockade of CD94/NKG2 markedly enhanced the antimetastatic effect of α-GalCer after α-GalCer priming. These findings revealed a negative feedback regulation of iNKT-cell activation by IFN-γ–inducible Qa-1$^b$ and provided a novel strategy to improve the antimetastatic effect of α-GalCer by priming with OCH or by blocking CD94/NKG2-mediated suppression.

It was unexpected that OCH was far more effective than α-GalCer in priming the secondary iNKT-cell responses to α-GalCer, since OCH and α-GalCer similarly modulated iNKT-cell surface receptors and OCH was rather inferior to α-GalCer in expanding iNKT cells upon priming (data not shown) as recently reported.[6,9] We hypothesized that IFN-γ produced by iNKT cells upon priming with α-GalCer might be responsible for this difference, since OCH did not induce IFN-γ production in vivo. We found that α-GalCer priming up-regulated the expression of Qa-1$^b$ in an IFN-γ–dependent manner, which suppressed iNKT-cell activation in response to secondary α-GalCer stimulation in vitro and in vivo. Qa-1$^b$ is an MHC class Ib molecule broadly expressed on leukocytes and it predominantly presents a canonical signal peptide of classical MHC class Ia molecules, called Qa-1 determinant modifier (Qdm), in a transporter associated with antigen presentation (TAP)–dependent manner, thereby indirectly representing cellular MHC class Ia levels.[32,33] The up-regulation of Qa-1$^b$ expression by IFN-γ might be due to increased transcription of *Qa-1$^b$* and/or increased TAP-mediated loading of Qdm onto Qa-1$^b$. The Qdm/Qa-1$^b$ complex is recognized by inhibitory CD94/NKG2A and activating CD94/NKG2C or E receptors.[21-23] The CD94/NKG2 receptors expressed on naive and primed iNKT cells were predominantly CD94/NKG2A as estimated by staining with an NKG2A-specific mAb as previously reported.[22] It has been shown that CD94/NKG2A expressed on NK cells and CD8$^+$ T cells suppressed their activation.[34] However, our present results are the first indication that iNKT-cell activation is critically regulated by CD94/NKG2A. Similarly, inhibitory Ly49 receptors, which recognize MHC class Ia molecules directly, have been reported to suppress α-GalCer–induced iNKT-cell activation.[30,35] Since CD94/NKG2A is more frequently expressed on iNKT cells than Ly49, it may play a more dominant role in regulating iNKT-cell activation. The IFN-γ–mediated Qa-1$^b$ up-regulation may be a negative feedback mechanism to maintain self-tolerance of iNKT cells and avoid a pathogenic effect of iNKT cells.[36-39] It will be interesting to explore the iNKT-cell functions in Qa-1$^b$–deficient[40] or CD94-deficient[22] mice in future studies.

Consistent with recent reports,[18-20] we observed a rapid down-modulation of TCR and NK1.1 on the surface of iNKT cells upon priming with their TCR ligands, which mostly accounted for the apparent disappearance of iNKT cells. However, intracellular staining 1 day after α-GalCer priming demonstrated a 20% to 30% reduction of iNKT-cell numbers compared with untreated mice (data not shown), and some annexin V–positive iNKT cells were detected in the liver and spleen promptly after α-GalCer injection as we reported previously.[16] Therefore, some minor fraction of iNKT cells appeared to be susceptible to AICD upon α-GalCer priming. A significant increase of CD94/NKG2$^+$ iNKT cells after α-GalCer priming suggested that these cells were more resistant to AICD than CD94/NKG2$^-$ iNKT cells. This preferential survival and/or expansion of CD94/NKG2$^+$ iNKT cells might be at least partly responsible for the higher sensitivity of primed iNKT cells to Qa-1$^b$ and CD94/NKG2-mediated suppression.

We and others have recently shown that the expansion of iNKT cells is maximal 3 days after α-GalCer priming and then iNKT-cell numbers gradually return to normal levels by homeostatic mechanisms within 7 to 10 days.[9,18-20] This is consistent with the kinetics of recall responses of α-GalCer– or OCH-primed mice to α-GalCer, suggesting that the enhanced secondary responses were mainly due to expansion of iNKT cells after priming. However, the enhanced secondary responses were mostly maintained up to 10 days after α-GalCer priming if CD94/NKG2-mediated suppression was blocked at the secondary α-GalCer stimulation. This suggests that the primed iNKT cells with a high capacity to produce cytokines upon restimulation persist (typical of effector/ memory T cells), although they are under a strict regulation by CD94/NKG2A-mediated suppression.

A recent study has shown that the recognition of α-GalCer analogues was influenced by the TCR Vβ repertoires of iNKT cells. OCH was preferentially recognized by Vβ8$^+$ iNKT cells, which also have a higher avidity for α-GalCer than Vβ7$^+$ iNKT cells.[7,41] Thus, a preferential expansion of Vβ8$^+$ iNKT cells after OCH or α-GalCer priming might also be responsible for the enhanced responses of primed iNKT cells to α-GalCer restimulation in vitro and in vivo.

We have previously shown that α-GalCer administration into naive mice induces sustained IFN-γ production and cytotoxic activity, which were mediated by NK cells secondarily activated by IFN-γ derived from iNKT cells and IL-12 derived from DCs.[16,29,31] Thus, depletion of NK cells mostly abrogated the sustained α-GalCer response and consequently impaired the antimetastatic effect of α-GalCer. In contrast, α-GalCer administration into OCH-primed mice induced a greatly enhanced IFN-γ production at 5 hours but not at 16 to 20 hours, which was not reduced by NK-cell depletion (data not shown). This indicated that OCH priming mainly enhanced IFN-γ production by iNKT cells themselves, rather that secondary activated NK cells, upon the secondary α-GalCer stimulation. However, the markedly enhanced cytotoxic activity of liver and spleen MNCs 24 hours after α-GalCer boost in OCH-primed mice was mostly abrogated by NK-cell depletion (K.T., unpublished data, May 2004). In addition, the

significantly augmented antimetastatic effect of α-GalCer in OCH-primed mice was significantly inhibited by NK-cell depletion (K.T., unpublished data, May 2004). These data suggested that IFN-γ–activated NK cells were mainly responsible for the antimetastatic effect of α-GalCer in the OCH-primed mice. In this context, the CD94/NKG2 blockade might augment the antimetastatic effect of α-GalCer by enhancing the activation of not only iNKT cells but also NK cells, since NK cells also express CD94/NKG2A inhibitory receptors. Thus, blockade of the CD94/NKG2A suppressive pathway may be effective at either the induction or effector phase of the α-GalCer–induced antitumor effect.

The most notable finding of this study is that the antimetastatic effect of α-GalCer was greatly improved by the OCH-priming or the CD94/NKG2A blockade. OCH was a weak inducer of iNKT-cell expansion and IL-4 production but did not induce IFN-γ production or antimetastatic activity by itself.[6,7,9] However, OCH modulated iNKT-cell surface receptors as efficiently as α-GalCer. These OCH-primed iNKT cells produced a huge amount of IFN-γ upon secondary α-GalCer restimulation in vivo, resulting in a potent antimetastatic effect. The inability of OCH to induce IFN-γ was a beneficial property for priming secondary α-GalCer responses because IFN-γ down-regulated the secondary iNKT-cell responses by up-regulating Qa-1$^b$ and thus CD94/NKG2A-mediated suppression. Recent studies have demonstrated quantitative and qualitative differences in the in vivo response of iNKT cells to distinct α-GalCer analogues, including OCH and β-GalCer.[9] Like OCH, in our preliminary experiments, priming with β-GalCer a26,[9] another weak iNKT-cell ligand inducing poor cytokine production, also potently enhanced iNKT-cell responses to α-GalCer restimulation (data not shown). α-GalCer and OCH have been shown to activate human Vα24 iNKT cells in a similar manner to murine Vα14 iNKT cells in vitro,[3,4] and α-GalCer is now in early clinical trials in cancer patients.[42,43] Therefore, priming with OCH may be a novel strategy to improve the therapeutic effect of α-GalCer in such patients. Further exploration of an α-GalCer analog with a better priming effect is also warranted. CD94/NKG2A blockade might be also applicable to improve the antitumor effect of α-GalCer in humans. In addition to an antitumor effect, α-GalCer has been shown to protect mice against infections and autoimmune diseases.[1-4,13,14] Therefore, the priming with OCH and the blockade of CD94/NKG2A may also be applicable to improve the therapeutic effect of α-GalCer in these diseases. However, it has also been shown that α-GalCer occasionally exacerbated autoimmune diseases, depending on the model and/or administration protocol.[44] Moreover, overactivation of iNKT cells can induce tissue pathologies.[36-39] Therefore, further studies are needed to determine the optimal prime/boost protocol or blockade of NK-cell receptors in iNKT-cell–targeting therapy for the safe treatment of tumor, infections, and autoimmune diseases.

## Acknowledgment

We thank Lewis L. Lanier for reading the manuscript and helpful suggestions.

## References


1. Bendelac A, Rivera MN, Park SH, Roark JH. Mouse CD1-specific NK1 T cells: development, specificity, and function. Annu Rev Immunol. 1997;15:535-562.
2. Godfrey DI, Hammond KJ, Poulton LD, Smyth MJ, Baxter AG. NKT cells: facts, functions and fallacies. Immunol Today. 2000;21:573-583.
3. Kronenberg M, Gapin L. The unconventional lifestyle of NKT cells. Nat Rev Immunol. 2002;2:557-568.
4. Taniguchi M, Harada M, Kojo S, Nakayama T, Wakao H. The regulatory role of Vα14 NKT cells in innate and acquired immune response. Annu Rev Immunol. 2003;21:483-513.
5. Kawano T, Cui J, Koezuka Y, et al. CD1d-restricted and TCR-mediated activation of Vα14 NKT cells by glycosylceramides. Science. 1997; 278:1626-1629.
6. Miyamoto K, Miyake S, Yamamura T. A synthetic glycolipid prevents autoimmune encephalomyelitis by inducing TH2 bias of natural killer T cells. Nature. 2001;413:531-534.
7. Stanic AK, Shashidharamurthy R, Bezbradica JS, et al. Another view of T cell antigen recognition: cooperative engagement of glycolipid antigens by Vα14Jα18 natural T(iNKT) cell receptor. J Immunol. 2003;171:4539-4551.
8. Ortaldo JR, Young HA, Winkler-Pickett RT, Bere EW Jr, Murphy WJ, Wiltrout RH. Dissociation of NKT stimulation, cytokine induction, and NK activation in vivo by the use of distinct TCR-binding ceramides. J Immunol. 2004;172:943-953.
9. Parekh VV, Singh AK, Wilson MT, et al. Quantitative and qualitative differences in the in vivo response of NKT cells to distinct α- and β-anomeric glycolipids. J Immunol. 2004;173:3693-3706.
10. Zhou D, Mattner J, Vantu III C, et al. Lysosomal glycosphingolipid recognition by NKT cells. Science. 2004;306:1786-1789.
11. Hayakawa Y, Takeda K, Yagita H, Van Kaer L, Saiki I, Okumura K. Differential regulation of Th1 and Th2 functions of NKT cells by CD28 and CD40 costimulatory pathways. J Immunol. 2001; 166:6012-6018.
12. Ikarashi Y, Mikami R, Bendelac A, et al. Dendritic cell maturation overrules H-2D-mediated natural killer T (NKT) cell inhibition: critical role for B7 in CD1d-dependent NKT cell interferon γ production. J Exp Med. 2001;194:1179-1186.
13. Smyth MJ, Godfrey DI. NKT cells and tumor immunity: a double-edged sword. Nat Immunol. 2000;1:459-460.
14. Smyth MJ, Crowe NY, Hayakawa Y, Takeda K, Yagita H, Godfrey DI. NKT cells: conductors of tumor immunity? Curr Opin Immunol. 2002;14: 165-171.
15. Eberl G, MacDonald HR. Rapid death and regeneration of NKT cells in anti-CD3ε- or IL-12-treated mice: a major role for bone marrow in NKT cell homeostasis. Immunity. 1998;9:345-353.
16. Hayakawa Y, Takeda K, Yagita H, et al. Critical contribution of IFN-γ and NK cells, but not perforin-mediated cytotoxicity, to anti-metastatic effect of α-galactosylceramide. Eur J Immunol. 2001;31:1720-1727.
17. Matsuda JL, Naidenko OV, Gapin L, et al. Tracking the response of natural killer T cells to a glycolipid antigen using CD1d tetramers. J Exp Med. 2000;192:741-754.
18. Wilson MT, Johansson C, Olivares-Villagómez D, et al. The response of natural killer T cells to glycolipid antigens is characterized by surface receptor down-modulation and expansion. Proc Natl Acad Sci U S A. 2003;100:10913-10918.
19. Crowe NY, Uldrich AP, Kyparissoudis K, et al. Glycolipid antigen drives rapid expansion and sustained cytokine production by NK T cells. J Immunol. 2003;171:4020-4027.
20. Harada M, Seino K, Wakao H, et al. Down-regulation of the invariant Vα14 antigen receptor in NKT cells upon activation. Int Immunol. 2004;16:241-247.
21. Vance RE, Jamieson AM, Raulet DH. Recognition of the class Ib molecule Qa-1$^b$ by putative activating receptors CD94/NKG2C and CD94/NKG2E on mouse natural killer cells. J Exp Med. 1999; 190:1801-1812.
22. Vance RE, Jamieson AM, Cado D, Raulet DH. Implications of CD94 deficiency and monoallelic NKG2A expression for natural killer cell development and repertoire formation. Proc Natl Acad Sci U S A. 2002;99:868-873.
23. Vance RE, Kraft JR, Altman JD, Jensen PE, Raulet DH. Mouse CD94/NKG2A is a natural killer cell receptor for the nonclassical major histocompatibility complex (MHC) class I molecule Qa-1$^b$. J Exp Med. 1998;188:1841-1848.
24. Tagawa Y, Sekikawa K, Iwakura Y. Suppression of concanavalin A-induced hepatitis in IFN-γ$^{-/-}$ mice, but not in TNF-α$^{-/-}$ mice: role for IFN-γ in activating apoptosis of hepatocytes. J Immunol. 1997;159:1418-1428.
25. Ogasawara K, Hamerman JA, Hsin H, et al. Impairment of NK cell function by NKG2D modulation in NOD mice. Immunity. 2003;18:41-51.
26. Tajima A, Tanaka T, Ebata T, et al. Blastocyst MHC, a putative murine homologue of HLA-G, protects TAP-deficient tumor cells from natural killer cell-mediated rejection in vivo. J Immunol. 2003;171:1715-1721.
27. Ruedl C, Rieser C, Bock G, Wick G, Wolf H. Phenotypic and functional characterization of CD11c$^+$ dendritic cell population in mouse Peyer's patches. Eur J Immunol. 1996;26:1801-1806.
28. Maldonado-Lopez R, De Smedt T, Michel P, et al. CD8α$^+$ and CD8α$^-$ subclasses of dendritic cells direct the development of distinct T helper cells in vivo. J Exp Med. 1999;189:587-592.
29. Kitamura H, Iwakabe K, Yahata T, et al. The natural killer T (NKT) cell ligand α-galactosylceramide demonstrates its immunopotentiating effect by inducing interleukin (IL)-12 production by dendritic cells and IL-12 receptor expression on NKT cells. J Exp Med. 1999;189:1121-1128.

30. Hayakawa Y, Berzins SP, Crowe NY, Godfrey DI, Smyth MJ. Antigen-induced tolerance by intrathymic modulation of self-recognizing inhibitory receptors. Nat Immunol. 2004;5:590-596.
31. Carnaud C, Lee D, Donnars O, et al. Cross-talk between cells of the innate immune system: NKT cells rapidly activate NK cells. J Immunol. 1999; 163:4647-4650.
32. Soloski MJ, DeCloux A, Aldrich CJ, Forman J. Structural and functional characteristics of the class Ib molecule, Qa-1. Immunol Rev. 1995;147: 67-89.
33. Aldrich CJ, DeCloux A, Woods AS, Cotter RJ, Soloski MJ, Forman J. Identification of a Tap-dependent leader peptide recognized by alloreactive T cells specific for a class Ib antigen. Cell. 1994;79: 649-658.
34. Vivier E, Anfossi N. Inhibitory NK-cell receptors on T cells: witness of the past, actors of the future. Nat Rev Immunol. 2004;4:190-198.
35. Maeda M, Lohwasser S, Yamamura T, Takei F. Regulation of NKT cells by Ly49: analysis of primary NKT cells and generation of NKT cell line. J Immunol. 2001;167:4180-4186.
36. Takeda K, Hayakawa Y, Van Kaer L, Matsuda H, Yagita H, Okumura K. Critical contribution of liver natural killer T cells to a murine model of hepatitis. Proc Natl Acad Sci U S A. 2000;97:5498-5503.
37. Osman Y, Kawamura T, Naito T, et al. Activation of hepatic NKT cells and subsequent liver injury following administration of α-galactosylceramide. Eur J Immunol. 2000;30:1919-1928.
38. Ito K, Karasawa T, Kawano T, et al. Involvement of decidual Vα14 NKT cells in abortion. Proc Natl Acad Sci U S A. 2000;97:740-744.
39. Tupin E, Nicoletti A, Elhage R, et al. CD1d-dependent activation of NKT cells aggravates atherosclerosis. J Exp Med. 2004;199:417-422.
40. Hu D, Ikizawa K, Lu L, Sanchirico ME, Shonohara ML, Cantor H. Analysis of regulatory CD8 T cells in Qa-1-deficient mice. Nat Immunol. 2004;5:516-523.
41. Schümann J, Voyle RB, Wei BY, MacDonald HR. Influence of the TCR Vβ domain on the avidity of CD1d:α-galactosylceramide binding by invariant Vα 14 NKT cells. J Immunol. 2003;170:5815-5819.
42. Giaccone G, Punt CJ, Ando Y, et al. A phase I study of the natural killer T-cell ligand α-galactosylceramide (KRN7000) in patients with solid tumors. Clin Cancer Res. 2002;8:3702-3709.
43. Nieda M, Okai M, Tazbirkova A, et al. Therapeutic activation of Vα24+Vβ11+ NKT cells in human subjects results in highly coordinated secondary activation of acquired and innate immunity. Blood. 2004;103:383-389.
44. Mars LT, Novak J, Liblau RS, Lehuen A. Therapeutic manipulation of iNKT cells in autoimmunity: modes of action and potent risks. Trends Immunol. 2004;25:471-476.

ARTHRITIS & RHEUMATISM
Vol. 52, No. 6, June 2005, pp 1941–1948
DOI 10.1002/art.21056


# The Involvement of $V_\alpha 14$ Natural Killer T Cells in the Pathogenesis of Arthritis in Murine Models

Asako Chiba, Shinjiro Kaieda, Shinji Oki, Takashi Yamamura, and Sachiko Miyake

*Objective.* To examine the physiologic role of natural killer T (NKT) cells bearing $V_\alpha 14$ T cell receptor (TCR) in the pathogenesis of collagen-induced arthritis (CIA) and antibody-induced arthritis in mice.

*Methods.* NKT cells were stained with α-galactosylceramide–loaded CD1 dimer, and then assessed using flow cytometry. CIA was induced in mice by immunization on days 0 and 21 with type II collagen (CII) emulsified with an equal volume of Freund's complete adjuvant. Anti-CII antibodies were measured by enzyme-linked immunosorbent assay. For antibody-induced arthritis, mice were injected with anti-CII monoclonal antibodies (mAb) followed by lipopolysaccharide, or with serum from KRN TCR–transgenic mice crossed with nonobese diabetic mice (K/BxN). The severity of arthritis was monitored with a macroscopic scoring system.

*Results.* The number of NKT cells increased in the liver at the peak of the clinical course of CIA. Administration of anti-CD1 mAb inhibited development of CIA. The severity of CIA in NKT cell–deficient mice was reduced compared with that in wild-type mice. The IgG1:IgG2a ratio of anti-CII was elevated and production of interleukin-10 from draining lymph node cells was increased in NKT cell–deficient mice. NKT cell–deficient mice were significantly less susceptible to antibody-induced arthritis.

*Conclusion.* NKT cells contribute to the pathogenesis of arthritis by enhancing autoantibody-mediated inflammation. NKT cells also contribute to the disease process in a deleterious way, due, at least in part, to the alteration of the Th1/Th2 balance in T cell response to CII.

Rheumatoid arthritis (RA) is a common autoimmune disease characterized by persistent inflammation of the joints. Affected joints display hyperplasia of the synovia with large cellular infiltrates of several cell types, including neutrophils, macrophages, T cells, B cells, dendritic cells, and fibroblasts. Complement deposition and high levels of proinflammatory cytokine expression are found in the synovial and periarticular regions, and the perpetuation of synovitis results in destruction of the cartilage and bone of the affected joints. Although the etiology of RA remains controversial, cumulative evidence suggests that T cell–mediated autoimmune responses play an important role, and the ensuing inflammation is a critical component in the processes leading to damage of joint cartilage and bone (1).

Natural killer T (NKT) cells are a unique subset of T cells that coexpress receptors of the NK lineage and α/β T cell receptor (TCR). A majority of NKT cells express an invariant TCRα chain (encoded by a $V_\alpha 14$–$J_\alpha 281$ rearrangement in mice and a homologous $V_\alpha 24$–$J_\alpha Q$ rearrangement in humans). Unlike conventional T cells that recognize peptides in association with the major histocompatibility complex (MHC), $V_\alpha 14$ NKT cells recognize glycolipid antigens such as α-galactosylceramide (α-GC) presented by the nonpolymorphic MHC class I–like protein, CD1d. $V_\alpha 14$ NKT cells have been demonstrated to regulate a variety of immune responses through their capacity to produce a large amount of cytokines, including interleukin-4 (IL-4) and interferon-γ (IFNγ), in response to TCR ligation or cytokine stimulation (2–4). Furthermore, we previously demonstrated that stimulation of $V_\alpha 14$ NKT cells with the glycolipid ligand, OCH, can inhibit collagen-induced arthritis (CIA), a murine experimental model for RA

Supported by a grant-in-aid for scientific research from the Japan Society for the Promotion of Science (B-14370169), the Uehara Memorial Foundation, the Kato Memorial Bioscience Foundation, and the Pharmaceutical and Medical Devices Agency.

Asako Chiba, MD, PhD, Shinjiro Kaieda, MD, Shinji Oki, PhD, Takashi Yamamura, MD, PhD, Sachiko Miyake, MD, PhD: National Institute of Neuroscience, Tokyo, Japan.

Address correspondence and reprint requests to Sachiko Miyake, MD, PhD, Department of Immunology, National Institute of Neuroscience, NCNP 4-1-1 Ogawahigashi, Kodaira, Tokyo 187-8502, Japan. E-mail: miyake@ncnp.go.jp.

Submitted for publication July 30, 2004; accepted in revised form March 1, 2005.

induced by immunization with type II collagen (CII), suggesting that $V_\alpha14$ NKT cells are a potential target for RA therapy (5).

Although the precise function of $V_\alpha14$ NKT cells remains to be elucidated, evidence indicates that $V_\alpha14$ NKT cells play a critical role in the regulation of autoimmune responses (6–8). Abnormalities in the numbers and function of $V_\alpha14$ NKT cells have been observed in patients with autoimmune diseases, including RA, as well as in a variety of mouse strains that are genetically predisposed to the development of autoimmune diseases (9–15). Despite these accumulating data, the role of $V_\alpha14$ NKT cells in the pathogenesis of arthritis still remains unclear.

In the present study, we show that blockade of CD1d results in the amelioration of CIA. In addition, the severity of CIA induced in $V_\alpha14$ NKT cell–deficient mice was reduced in comparison with that in wild-type mice, due to a reduction in the Th1 deviation of T cell responses to CII. Furthermore, mice deficient in $V_\alpha14$ NKT cells were significantly less susceptible to antibody-induced arthritis, indicating that $V_\alpha14$ NKT cells also contribute to autoantibody-mediated inflammation.

## MATERIALS AND METHODS

**Mice.** DBA1/J mice were purchased from Oriental Yeast Co., Ltd (Tokyo, Japan). C57BL/6 (B6) mice were purchased from Clea Laboratory Animal Corporation (Tokyo, Japan). $J_\alpha281$-knockout mice were kindly provided by Dr. Masaru Taniguchi (Riken Research Center for Allergy and Immunology, Yokohama, Japan) (16), and were generated in the 129 strain and backcrossed 10 times to the B6 background. CD1-knockout mice were kindly provided by Dr. Steve B. Balk (Beth Israel Deaconess Medical Center, Harvard Medical School, Boston, MA) (17), and were generated in the 129 strain and backcrossed 7 times to the B6 background. KRN TCR–transgenic mice were kindly provided by Drs. Christophe Benoist and Diane Mathis (Joslin Diabetes Center, Boston, MA) (18). The animals were kept under specific pathogen–free conditions.

**Flow cytometric analysis of NKT cells.** Cells were prepared from various organs of control DBA1/J mice and CIA mice at 30–35 days after the first immunization. Control mice were injected intradermally with vehicle alone emulsified in Freund's complete adjuvant (CFA) at day 0 and in Freund's incomplete adjuvant (IFA) at day 21. Dimer XI Recombinant Soluble Dimetric Mouse CD1d, fluorescein isothiocyanate–conjugated A85-1 monoclonal antibodies (mAb) (anti-mouse IgG1), and allophycocyanin-conjugated anti-TCR$\beta$ chain were purchased from BD Biosciences PharMingen (San Diego, CA). Loading of $\alpha$-GC to CD1d and staining for Dimer XI were achieved in accordance with the manufacturer's protocol. Flow cytometric analysis was performed with FACSCaliber flow cytometry (Becton Dickinson Immunocytometry Systems, Mountain View, CA).

**Induction of CIA.** Mice were immunized intradermally at the base of the tail with either 200 $\mu$g of bovine CII (for DBA1/J mice) or 100 $\mu$g of chicken CII (for B6 mice) (Collagen Research Center, Tokyo, Japan) emulsified with an equal volume of CFA and containing 250 $\mu$g of H37Ra *Mycobacterium tuberculosis* (Difco, Detroit, MI). B6 mice received a booster by intradermal injection with the same antigen preparation on day 21. DBA1/J mice received a booster by intradermal injection with 200 $\mu$g of bovine CII emulsified with IFA.

**Induction of anti-CII antibody–induced arthritis.** Mice were injected intravenously with 2 mg of the mixture of anti-CII mAb (Arthrogen-CIA mAb; Chondrex, Seattle, WA), and 3 days later, 50 $\mu$g of lipopolysaccharide (LPS) was injected intraperitoneally. Control mice were injected with mouse IgG (Sigma, St. Louis, MO) followed by LPS injection.

**Induction of arthritis by K/BxN serum transfer.** As previously described, KRN TCR–transgenic mice maintained on the B6 background were crossed with nonobese diabetic (NOD) mice to generate K/BxN mice that develop spontaneous arthritis (18). K/BxN serum pools were prepared from 8-week-old, arthritic mice, and 200 $\mu$l of the serum was injected intraperitoneally into the animals to induce arthritis. Sera from nontransgenic littermate mice crossed with NOD mice (BxN) were used as the control.

**Clinical assessment of arthritis.** Mice were examined for signs of joint inflammation, using the following scoring system: 0 = no change, 1 = significant swelling and redness of 1 digit, 2 = mild swelling and erythema of the limb or swelling of >2 digits, 3 = marked swelling and erythema of the limb, and 4 = maximal swelling and redness of the limb and subsequent ankylosis. The average of the macroscopic score was expressed as the cumulative value of all paws, with a maximum possible score of 16.

**In vivo antibody treatment.** Anti-CD1–blocking, non–cell-depleting mAb (1B1) was purchased from BD Biosciences PharMingen (19). Mice were treated intraperitoneally with 250 $\mu$g of either blocking anti-CD1d mAb or non–isotype-matched whole rat IgG (Sigma) as control, twice per week starting from 21 days after the first immunization with CII.

**Measurements of CII-specific IgG1 and IgG2a.** Either chicken or bovine CII (1 mg/ml) was coated onto enzyme-linked immunosorbent assay plates (Sumitomo Bakelite, Tokyo, Japan) at 4°C overnight. After blocking with 1% bovine serum albumin in phosphate buffered saline, serially diluted serum samples were added to CII-coated wells. For detection of anti-CII antibodies, the plates were incubated for 1 hour with biotin-labeled anti-IgG1 and anti-IgG2a (Southern Biotechnology Associates, Birmingham, AL) or anti-IgG antibodies (CN/Cappel, Aurora, OH) and then incubated with streptavidin-peroxidase. After adding a substrate, the reaction was evaluated, and antibody titers were calculated on the basis of dilution/absorbance curves.

**Cytokine measurement.** B6 or $J_\alpha281$-knockout mice were immunized with 100 $\mu$g of CII on days 0 and 21. Ten days after the second immunization, the lymph node cells from B6 or $J_\alpha281$-knockout mice were cultured for 48 hours with 200 $\mu$g/ml CII. The levels of IL-2, IL-4, IL-5, IL-10, IFN$\gamma$, and tumor necrosis factor $\alpha$ (TNF$\alpha$) in the supernatants were measured by cytometric bead array (BD PharMingen), using the protocol provided by the manufacturer.

**Histopathology.** B6 or $J_\alpha281$-knockout mice were killed and the fore paws removed 65 days after the induction of CIA or 10 days after K/BxN serum transfer. Paws were then fixed in buffered formalin, decalcified, embedded in paraffin, sectioned, and stained with hematoxylin and eosin.

## RESULTS

**Increase in liver NKT cells in CIA.** To investigate the role of CD1-restricted $V_\alpha14$ NKT cells in CIA, we first analyzed the number of $V_\alpha14$ NKT cells using α-GC–loaded CD1 dimer. As shown in Figure 1A, the percentage of α-GC–loaded CD1-reactive $V_\alpha14$ NKT cells among total liver mononuclear cells and peripheral blood mononuclear cells (PBMCs) was increased in CIA mice compared with control mice treated with CFA alone. The absolute number of α-GC–loaded CD1-reactive $V_\alpha14$ NKT cells was also increased in the liver at the peak of the disease (Figure 1B).

**Amelioration of CIA by anti-CD1 mAb treatment.** To elucidate the role of $V_\alpha14$ NKT cells in the pathogenesis of arthritis, we next examined the effect of anti-CD1d mAb on the development of CIA. We immunized DBA1/J mice and then administered intraperitoneal injections of either anti-CD1d mAb or control rat IgG twice per week starting from the day of the second immunization (5). As shown in Figure 2A, anti-CD1d treatment ameliorated arthritis in the mAb treatment

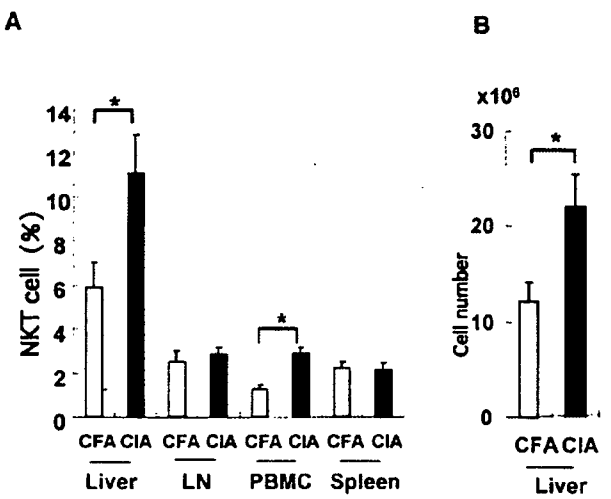


Figure 1. Expression of natural killer T (NKT) cells in the collagen-induced arthritis (CIA) model. A, To determine the frequency of NKT cells in various organs of mice with CIA or control mice (treated with Freund's complete adjuvant [CFA]), cells were obtained from the mice at the time of death, 30–35 days after the first immunization. Results are expressed as the percentage of α-galactosylceramide–loaded CD1d-positive T cells within the lymphocyte gates. LN = lymph nodes; PBMC = peripheral blood mononuclear cells. B, Absolute numbers of NKT cells in the liver were calculated from the total liver mononuclear cells of the same mice as in A. Bars show the mean and SEM of 7–8 mice per group. * = $P < 0.05$, by Mann-Whitney U test.

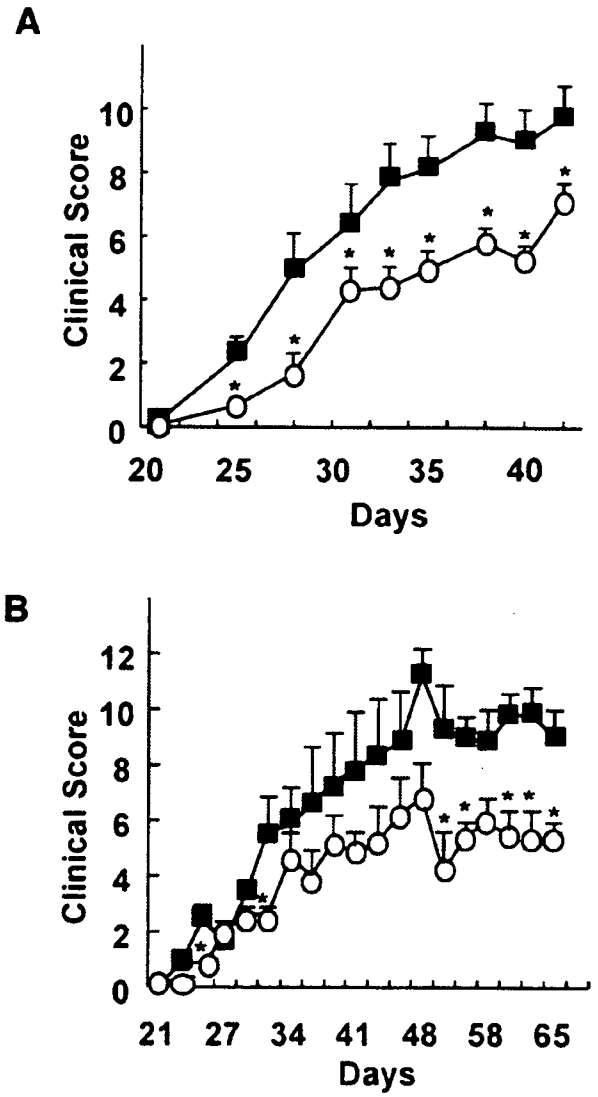


Figure 2. Amelioration of collagen-induced arthritis (CIA) in A, anti-CD1 monoclonal antibody (mAb)–treated or B, natural killer T cell–deficient mice. A, The clinical course of CIA was monitored in DBA/1 mice treated with 250 μg of anti-CD1d mAb (○) or control rat IgG (■), twice per week starting from day 21 after the first immunization. Bars show the mean and SEM of 13 mice (6-week-old males) per group from 2 independent experiments (n = 5 or 8 per group). * = $P < 0.05$ versus control IgG-treated mice, by Mann-Whitney U test. B, The clinical course of CIA was monitored in $J_\alpha281$-knockout (○) and wild-type B6 (■) mice immunized with chicken type II collagen emulsified with Freund's complete adjuvant. Bars show the mean and SEM of 5 mice per group. * = $P < 0.05$ versus B6 mice, by Mann-Whitney U test.

group as compared with that in the control group. Disease susceptibility was not different between anti-CD1d–treated mice and control mice. This result suggests that CD1d-restricted $V_\alpha14$ NKT cells contribute to the enhancement of the disease course in CIA.

**Reduced severity of CIA in NKT cell–deficient mice.** To further investigate the contribution of CD1-restricted $V_\alpha14$ NKT cells to arthritis, we induced CIA in $V_\alpha14$ NKT cell–deficient $J_\alpha281$-knockout mice. As shown in Figure 2B, $V_\alpha14$ NKT cell–deficient mice developed less severe arthritis compared with that in the wild-type B6 mice. Disease susceptibility was not different between B6 mice and $J_\alpha281$-knockout mice. This result further supports the idea that $V_\alpha14$ NKT cells could play a role in the enhancement of CIA.

**Altered CII-specific responses in NKT cell–deficient mice.** To examine whether the response to CII was altered in the presence or absence of $V_\alpha14$ NKT cells, we measured CII-specific IgG isotype levels 65 days after the induction of CIA. It is generally accepted that elevation of autoantigen-specific IgG2a antibody is the result of augmentation of the Th1 immune response to the antigen, whereas a higher level of IgG1 antibody is a reflection of a stronger Th2 response to the antigen. In $J_\alpha281$-knockout mice, there was a slight reduction in the level of antigen-specific IgG2a antibody and an increase in the level of antigen-specific IgG1 compared with that in wild-type B6 mice (Figure 3A). Consequently, the IgG1:IgG2a ratio was elevated in $J_\alpha281$-knockout mice, suggesting that $V_\alpha14$ NKT cell deficiency alters the Th1/Th2 balance in response to CII.

To further analyze the CII-reactive T cell response, we isolated the draining lymph node cells from B6 or $J_\alpha281$-knockout mice 10 days after the second immunization with CII, and stimulated the lymphoid cells with CII in vitro. We then compared the concentrations of IL-2, IL-4, IL-5, IL-10, IFNγ, and TNFα in the culture supernatants. The level of IL-10 was significantly increased in the supernatant obtained from the culture of lymphoid cells of $J_\alpha281$-knockout mice compared with those from B6 mice (Figure 3B). The concentrations of IL-2 and IFNγ were decreased in $J_\alpha281$-knockout mice; however, the levels of these cytokines were also very low in B6 mice. The concentration of TNFα was not different between these mice. IL-4 and IL-5 were not detected in either culture supernatant. These results suggest that $V_\alpha14$ NKT cells contribute to the alteration of the Th1/Th2 balance of the T cell response to CII.

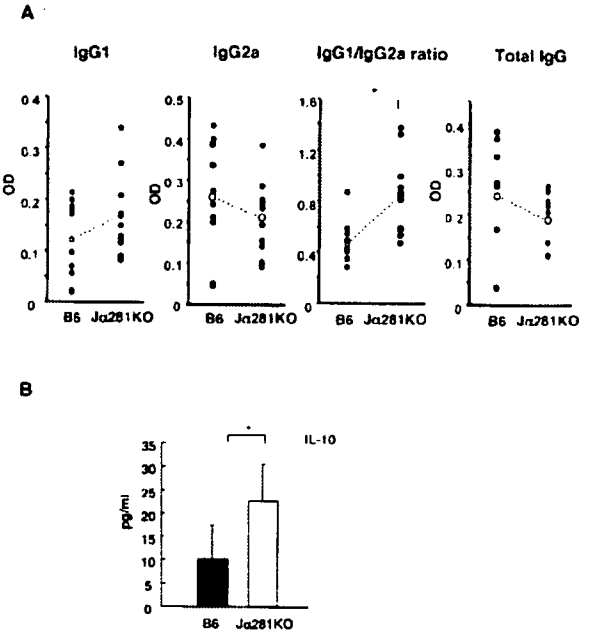


Figure 3. Altered type II collagen (CII)–specific responses in natural killer T cell–deficient mice. A, To determine the CII-specific antibody isotype levels in $J_\alpha281$-knockout (Jα281KO) mice as compared with wild-type B6 mice, individual serum samples obtained on day 65 after induction of arthritis were analyzed by enzyme-linked immunosorbent assay, with results expressed as the optical density (OD). Open circles with broken lines denote the average of individual samples. * = $P < 0.05$, by Student's *t*-test. B, To determine the CII-specific T cell response in Jα281KO as compared with wild-type B6 mice, production of interleukin-10 (IL-10) (among other cytokines) from draining lymph node cells was analyzed by cytometric bead array. Bars show the mean and SEM of 3 mice per group. * = $P < 0.05$, by Mann-Whitney U test.

**Amelioration of antibody-induced arthritis in NKT cell–deficient mice.** CIA, commonly used as a model of RA, is characterized both by a primary immune response and by inflammation, and these features are often interdependent and therefore difficult to separate. In antibody-induced arthritis, inflammation occurs in the absence of a primary immune response, allowing us to investigate the effector mechanisms that link the potentially pathogenic antibodies and the overt development of arthritis (20). To address the role of $V_\alpha14$ NKT cells in the inflammatory process in addition to the modulation of the T cell response, we studied the role of $V_\alpha14$ NKT cells in anti-CII antibody–induced arthritis. To induce arthritis, mice received a mixture of 4 mAb reactive to CII, followed 72 hours later by LPS. As shown in Figure 4, compared with that in control animals, the severity of joint inflammation was signifi-

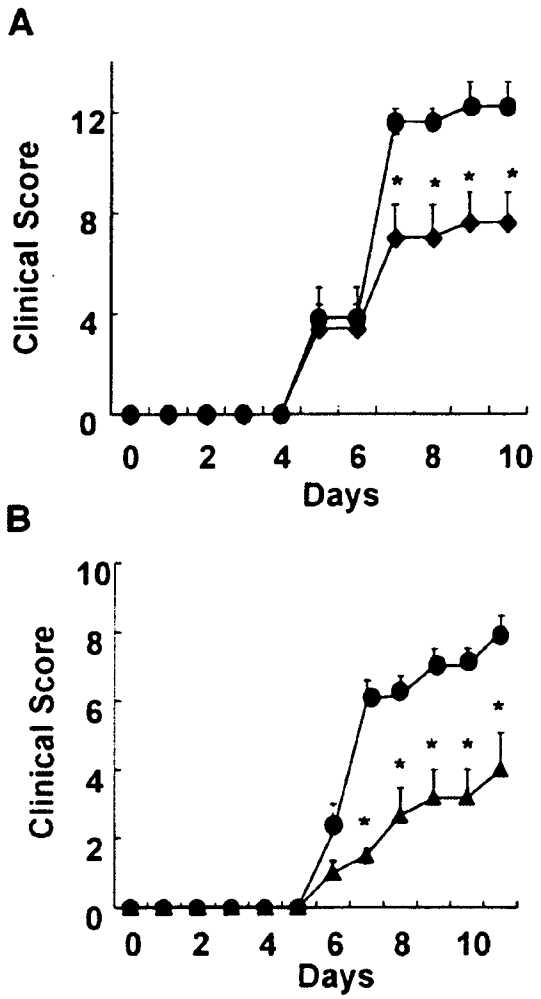


Figure 4. Reduced severity of anti–type II collagen monoclonal antibody (anti-CII mAb)–induced arthritis in natural killer T cell–deficient mice. The clinical course of arthritis induced by injection of a mixture of anti-CII mAb and lipopolysaccharide was monitored in 7-week-old female A, $J_\alpha 281$-knockout mice (◆) and B, CD1-knockout mice (▲) as compared with B6 mice (● in A and B). Bars show the mean and SEM of 5 mice per group, with representative data from 1 of 2 experiments. * = $P < 0.05$ versus B6 mice, by Mann-Whitney U test.

cantly reduced in $J_\alpha 281$-knockout mice as well as in CD1d-knockout mice, another NKT cell–deficient type of mouse (17). Disease susceptibility was not different among these 3 groups.

Arthritis induced by K/BxN serum transfer is another antibody-induced arthritis model (21). K/BxN is a recently developed model of inflammatory arthritis (18). K/BxN animals spontaneously develop arthritis

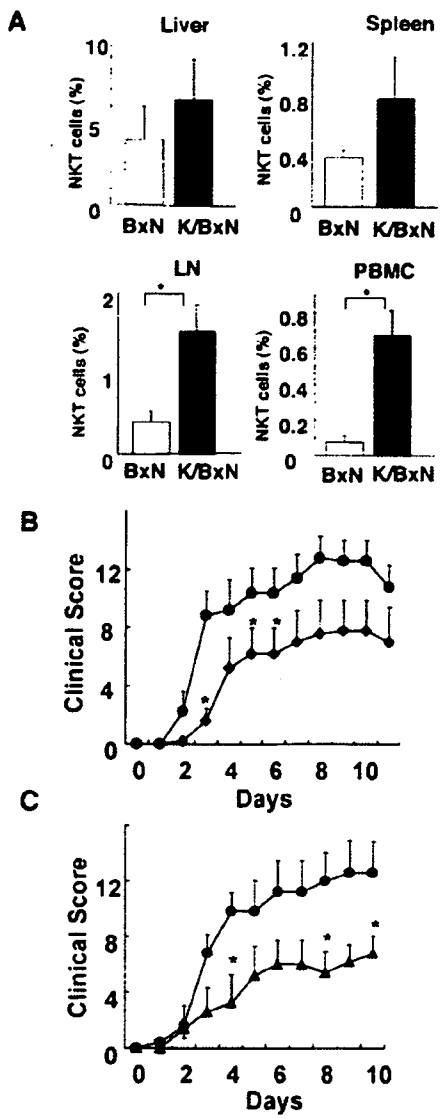


Figure 5. Reduced severity of arthritis induced by transfer of K/BxN serum in natural killer T (NKT) cell–deficient mice. A, To determine the frequency of NKT cells in various organs of mice with K/BxN serum–induced arthritis or BxN serum–transferred control mice, cells were obtained from the mice at the time of death, 10 days after serum transfer. Results are expressed as the percentage of α-galactosylceramide–loaded CD1-positive T cells within the lymphocyte gates. Bars show the mean and SEM of 3 mice per group. * = $P < 0.05$, by Mann-Whitney U test. LN = lymph nodes; PBMC = peripheral blood mononuclear cells. B and C, The clinical course of arthritis induced by the injection of K/BxN serum was monitored in 8-week-old female B, $J_\alpha 281$-knockout mice (◆) and C, CD1-knockout mice (▲) as compared with B6 mice (● in B and C). Bars show the mean and SEM of 5 mice per group, with representative data from 1 of 2 experiments. * = $P < 0.05$, by Mann-Whitney U test.

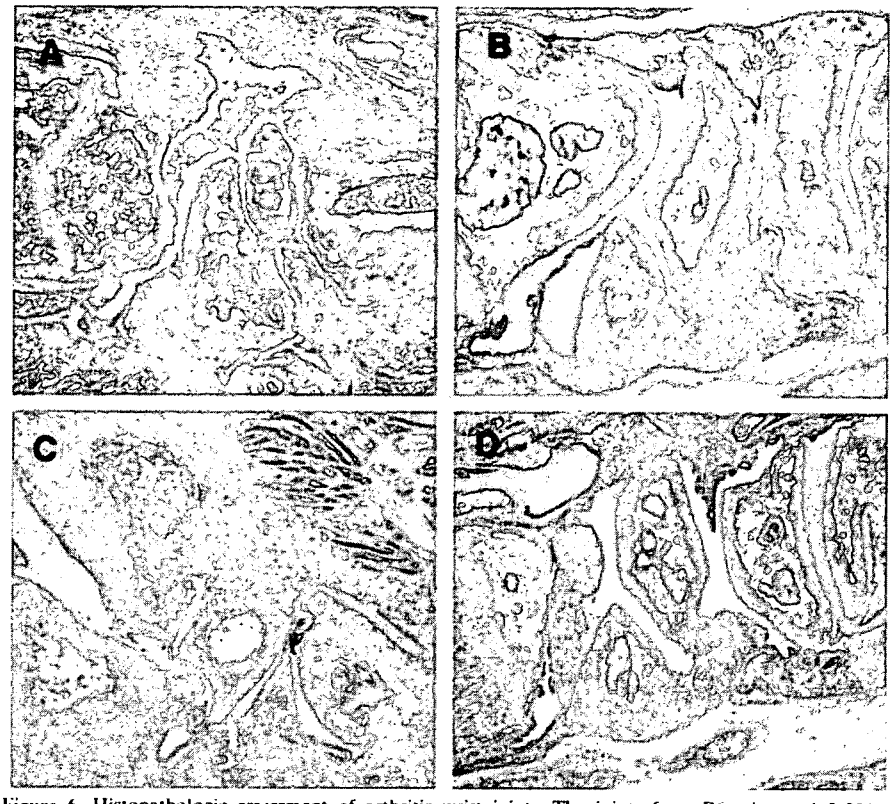


Figure 6. Histopathologic assessment of arthritic wrist joints. The joints from B6 mice and $J_\alpha$281-knockout mice with collagen-induced arthritis (A and B, respectively) and from B6 mice and $J_\alpha$281-knockout mice with K/BxN serum–transferred arthritis (C and D, respectively) were assessed for the extent of arthritis. Two mice per group were analyzed, and representative results are shown. (Hematoxylin and eosin stained; original magnification × 20.)

that is similar to RA in humans. The arthritis is initiated by T and B cell autoreactivity to a ubiquitously expressed antigen, glucose-6-phosphate-isomerase (GPI) (22). Transfer of serum from arthritic K/BxN mice into healthy animals provokes arthritis within days, independent of the response of T and B cells. K/BxN serum–induced arthritis is mediated by anti-GPI IgG.

With this arthritis model, we analyzed the number of $V_\alpha$14 NKT cells, utilizing α-GC–loaded CD1 dimer. As shown in Figure 5A, the percentage of α-GC–loaded CD1-restricted $V_\alpha$14 NKT cells among lymph node cells and PBMCs in arthritic mice was increased compared with that in control mice transferred with BxN serum. CD1-restricted $V_\alpha$14 NKT cells among total liver mononuclear cells and splenocytes tended to be increased in arthritic mice. As shown in Figures 5B and C, the severity of joint inflammation was significantly reduced in $J_\alpha$281-knockout mice and CD1d-knockout mice, respectively, as compared with that in control animals, which is consistent with the results observed in anti-CII antibody–induced arthritis. Disease susceptibility was not different among these 3 groups. These results indicate that $V_\alpha$14 NKT cells contribute to the inflammatory effector phase of arthritis.

**Histopathologic assessment of arthritis in $J_\alpha$281-knockout mice.** In addition to visual scoring of disease severity, we analyzed the histologic features in the joints of the fore paws of $J_\alpha$281-knockout mice and wild-type B6 mice on day 65 after CIA induction or 10 days after K/BxN serum transfer. As shown in Figure 6A, following arthritis development in B6 mice, there was severe disease in the joints, associated with massive cell infiltration, cartilage erosion, and bone destruction. These histologic features were significantly less apparent in $J_\alpha$281-knockout mice (Figure 6B). In K/BxN serum–transferred B6 mice, massive cell infiltration as well as

cartilage erosion and bone destruction were observed (Figure 6C). Infiltration of inflammatory cells was less evident and destruction of cartilage and bone were not apparent in $J_\alpha$281-knockout mice (Figure 6D). These results support the idea that loss of $V_\alpha$14 NKT cells ameliorates arthritis.

## DISCUSSION

In this study, we demonstrated that blocking the interaction of CD1d and $V_\alpha$14 NKT cells leads to the amelioration of CIA. We also showed that the severity of the disease induced in $V_\alpha$14 NKT cell–deficient $J_\alpha$281-knockout mice was reduced compared with that in wild-type B6 mice. In $J_\alpha$281-knockout mice, the ratio of IgG1:IgG2a anti-CII antibody was elevated and production of IL-10 upon stimulation with CII was increased, suggesting that the response to CII was deviated to the Th2 response in these mice. Furthermore, we found that the disease was less severe in $J_\alpha$281- and CD1-knockout mice with antibody-induced arthritis.

The most extensively used animal model of RA is CIA, which is accompanied by a predominant Th1 response and is characterized by production of the proinflammatory cytokines IFNγ and TNFα. Previous studies have shown that treatment with Th2-promoting cytokines or with mAb directed against Th1-promoting cytokines can effectively protect mice against CIA (23). $V_\alpha$14 NKT cells were previously reported to protect other Th1 cell–mediated autoimmune diseases such as type I diabetes in NOD mice, by inducing a shift toward a Th2 T cell response to autoantigens (6–8). The development of diabetes was prevented either by infusion of NKT cell–enriched thymocyte preparations or by an increase of NKT cells in $V_\alpha$14–$J_\alpha$281–transgenic NOD mice (24,25). In contrast, $V_\alpha$14 NKT cells appeared to exacerbate arthritis in the present study, since the severity of the disease was decreased in $J_\alpha$281-knockout mice and anti-CD1d mAb treatment ameliorated the disease.

Because $V_\alpha$14 NKT cells produce large amounts of both IL-4 and IFNγ upon stimulation with anti-CD3 antibody or its prototypic ligand α-GC, a regulatory role in Th cell differentiation has been proposed for these cells. However, the results obtained from α-GC treatment of B6 mice on Th cell differentiation are conflicting. The administration of α-GC was found to facilitate either Th1 differentiation or Th2 differentiation (26,27). Although the basis for these inconsistencies is not clear, the discrepancies between these results could be due to the differences in the protocols of the α-GC treatment, suggesting that small differences in circumstances may affect the immunomodulatory effect of $V_\alpha$14 NKT cells. Recently, microbial products or proinflammatory cytokines such as IL-12 have been reported to amplify the basal weak responses of CD1d-restricted T cells to self antigens to yield potent effector functions by enhancing IFNγ secretion (28). Abundant proinflammatory cytokines may modulate the function of $V_\alpha$14 NKT cells in mice with CIA.

Recent studies using the serum of an engineered mouse model, K/BxN, have revealed that autoantibodies, complement components, Fc receptors, and cytokines such as IL-1 and TNFα participate in the pathogenesis of antibody-mediated erosive arthritis (29–31). As cellular components, neutrophils and mast cells have been reported to be essential for antibody-mediated inflammatory arthritis (32,33). We showed, in this study, that mice deficient in $V_\alpha$14 NKT cells exhibited a reduced severity of antibody-mediated arthritis, suggesting that $V_\alpha$14 NKT cells act as effector cells in inflammatory arthritis. Potential $V_\alpha$14 NKT cell effector mechanisms that may be important for the induction and progression of joint inflammation include the rapid production of a variety of cytokines, including IL-1 and TNFα, that play a critical role in both K/BxN serum–induced arthritis and anti-CII mAb–induced arthritis, as well as in human RA (1,30,31,34). Very recently, Kim et al reported that NKT cells promote K/BxN serum–induced joint inflammation by producing IL-4 and IFNγ (35). Those authors showed that IL-4 and IFNγ are important in reducing the production of transforming growth factor β (TGFβ), resulting in suppression of arthritis. The regulation of TGFβ by NKT cells might be one of the important mechanisms controlling the inhibition of arthritis.

In this study we have demonstrated that $V_\alpha$14 NKT cells could contribute to the pathogenesis of arthritis in several ways, including enhancing the inflammatory effector phase of arthritis mediated by autoantibodies. Changing the Th1/Th2 balance of autoantigen-reactive T cells by $V_\alpha$14 NKT cells may also contribute to the pathogenesis of CIA. As we previously proposed, modulation of the function of $V_\alpha$14 NKT cells with proper stimuli, such as the Th2-skewing glycolipid ligand, OCH, or a blocking reagent for NKT cell functions, could be considered as new therapeutic interventions in the management of RA.

## ACKNOWLEDGMENTS

We thank Masaru Taniguchi at the Riken Research Center for Allergy and Immunology for providing the $J_\alpha$281-

knockout mice, Steven Balk at Beth Israel Deaconess Medical Center and Harvard Medical School for providing the CD1-knockout mice, and Drs. Christophe Benoist and Diane Mathis, Joslin Diabetes Center and Harvard Medical School and Institu de Genetique et de Biologie Moleculaire et Cellulaire for providing the TCR-transgenic mice. We also thank Miho Mizuno and Chiharu Tomi for excellent technical assistance. We are grateful to John Ludvic Croxford for critical reading of the manuscript.

## REFERENCES

1. Feldmann M, Brennan FM, Maini RN. Role of cytokines in rheumatoid arthritis. Annu Rev Immunol 1996;14:397–440.
2. Brenner MB, Brigl M. CD1: antigen presentation and T cell function. Annu Rev Immunol 2004;22:817–90.
3. Taniguchi M, Harada M, Kojo S, Nakayama T, Wakao H. The regulatory role of Vα14 NKT cells in innate and acquired immune response. Annu Rev Immunol 2003;21:483–513.
4. Kronenberg M, Gapin L. The unconventional lifestyle of NKT cells. Nat Rev Immunol 2002;2:557–68.
5. Chiba A, Oki S, Miyamoto K, Hashimoto H, Yamamura T, Miyake S. Suppression of collagen-induced arthritis by natural killer T cell activation with OCH, a sphingosine-truncated analog of α-galactosylceramide. Arthritis Rheum 2004;50:305–13.
6. Hammond KJ, Godfrey DI. NKT cells: potential targets for autoimmune disease therapy? Tissue Antigens 2002;59:353–63.
7. Wilson SB, Delovitch TL. Janus-like role of regulatory iNKT cells in autoimmune disease and tumour immunity. Nat Rev Immunol 2003;3:211–22.
8. Hammond KJ, Kronenberg M. Natural killer T cells: natural or natural regulators of autoimmunity? Curr Opin Immunol 2003;15:683–9.
9. Sumida T, Sakamoto A, Murata H, Makino Y, Takahashi H, Yoshida S, et al. Selective reduction of T cells bearing invariant Vα24JαQ antigen receptor in patients with systemic sclerosis. J Exp Med 1995;182:1163–8.
10. Wilson SB, Kent SC, Patton KT, Orban T, Jackson RA, Exley M, et al. Extreme Th1 bias of invariant Vα24JαQ T cells in type 1 diabetes. Nature 1998;391:177–81.
11. Illes Z, Kondo T, Newcombe J, Oka N, Tabira T, Yamamura T. Differential expression of NK T cell Vα24JαQ invariant TCR chain in the lesions of multiple sclerosis and chronic inflammatory demyelinating polyneuropathy. J Immunol 2000;164:4375–81.
12. Kojo S, Adachi Y, Keino H, Taniguchi M, Sumida T. Dysfunction of T cell receptor AV24AJ18+, BV11+ double-negative regulatory natural killer T cells in autoimmune diseases. Arthritis Rheum 2001;44:1127–38.
13. Yoshimoto T, Bendelac A, Hu-Li J, Paul WE. Defective IgE production by SJL mice is linked to the absence of CD4+, NK1.1+ T cells that promptly produce interleukin 4. Proc Natl Acad Sci U S A 1995;92:11931–4.
14. Mieza MA, Itoh T, Cui JQ, Makino Y, Kawano T, Tsuchida K, et al. Selective reduction of Vα14+ NK T cells associated with disease development in autoimmune-prone mice. J Immunol 1996;156:4035–40.
15. Gombert JM, Herbelin A, Tancrede-Bohin E, Dy M, Carnaud C, Bach JF. Early quantitative and functional deficiency of NK1$^+$-like thymocytes in the NOD mouse. Eur J Immunol 1996;26:2989–98.
16. Cui J, Shin T, Kawano T, Sato H, Kondo E, Toura I, et al. Requirement for Vα14 NKT cells in IL-12-mediated rejection of tumors. Science 1997;278:1623–6.
17. Sonoda KH, Exley M, Snapper S, Balk SP, Stein-Streilein J. CD1-reactive natural killer T cells are required for development of systemic tolerance through an immune-privileged site. J Exp Med 2003;3:211–22.
18. Kouskoff V, Korganow AS, Duchatelle V, Degott C, Benoist C, Mathis D. Organ-specific disease provoked by systemic autoimmunity. Cell 1996;87:811–22.
19. Szalay G, Ladel CH, Blum C, Brossay L, Kronenberg M, Kaufmann SH. Anti-CD1 monoclonal antibody treatment reverses the production patterns of TGF-β2 and Th1 cytokines and ameliorates listerosis in mice. J Immunol 1999;162:6955–8.
20. Terato K, Hasty KA, Reife RA, Cremer MA, Kang H, Stuart JM. Induction of arthritis with monoclonal antibodies to collagen. J Immunol 1992;148:2103–8.
21. Korganow AS, Ji H, Mangialaio S, Duchatelle V, Pelanda R, Martin T, et al. From systemic T cell self-reactivity to organ-specific autoimmune disease via immunoglobulins. Immunity 1999;10:451–61.
22. Matsumoto I, Staub A, Benoist C, Mathis D. Arthritis provoked by linked T and B cell recognition of a glycolytic enzyme. Science 1999;286:1732–5.
23. Van Roon JA, Lafeber FP, Bijlsma JW. Synergistic activity of interleukin-4 and interleukin-10 in suppression of inflammation and joint destruction in rheumatoid arthritis [review]. Arthritis Rheum 2001;44:3–12.
24. Hammond KJ, Poulton LD, Palmisano LJ, Silveria PA, Godfrey DJ, Baxter AG. α/β-T cell receptor+CD4−CD8− (NKT) thymocytes prevent insulin-dependent diabetes mellitus in nonobese diabetic (NOD)/Lt mice by the influence of interleukin (IL)-4 and/or IL-10. J Exp Med 1998;187:1047–56.
25. Lehuen A, Lantz O, Beaudoin L, Laloux V, Carnaud C, Bendelac A, et al. Overexpression of natural killer T cells protects Vα14-Jα281 transgenic nonobese diabetic mice against diabetes. J Exp Med 1998;188:1831–9.
26. Singh N, Hong S, Scherer DC, Serizawa I, Burdin N, Kronenberg M, et al. Activation of NKT cells by CD1d and α-galactosylceramide directs conventional T cells to the acquisition of a Th2 phenotype. J Immunol 1999;163:2373–7.
27. Cui J, Watanabe N, Kawano T, Yamashita M, Kamata T, Shimizu C, et al. Inhibition of T helper cell type 2 cell differentiation and immunoglobulin E response by ligand-activated Vα14 natural killer T cells. J Exp Med 1999;190:783–92.
28. Brigl M, Bry L, Kent SC, Gumperz JE, Brenner MB. Mechanism of CD1d-restricted natural killer T cell activation during microbial infection. Nat Immunol 2003;12:1230–7.
29. Ji H, Ohmura K, Mahmood U, Lee DM, Hofhuis FM, Boackle SA, et al. Arthritis critically dependent on innate immune system players. Immunity 2002;16:157–68.
30. Kagari T, Doi H, Shimozato T. The importance of IL-1β and TNF-α, and the noninvolvement of IL-6, in the development of monoclonal antibody-induced arthritis. J Immunol 2002;169:1459–66.
31. Ji H, Pettit A, Ohmura K, Ortiz-Lopez A, Duchatelle V, Degott C, et al. Critical roles for interleukin 1 and tumor necrosis factor α in antibody-induced arthritis. J Exp Med 2002;196:77–85.
32. Wipke BT, Allen PM. Essential role of neutrophils in the initiation and progression of a murine model of rheumatoid arthritis. J Immunol 2001;167:1601–8.
33. Lee DM, Friend DS, Gurish MF, Benoist C, Mathis D, Brenner MB. Mast cells: a cellular link between autoantibodies and inflammatory arthritis. Science 2002;297:1689–92.
34. Oki S, Chiba A, Yamamura T, Miyake S. The clinical implication and molecular mechanism of preferential IL-4 production by modified glycolipid-stimulated NKT cells. J Clin Invest 2004;113:1631–40.
35. Kim HY, Kim HJ, Min HS, Kim S, Park WS, Park SH, et al. NKT cells promote antibody-induced joint inflammation by suppressing transforming growth factor β1 production. J Exp Med 2005;201:41–7.

# NKT Cells Are Critical for the Initiation of an Inflammatory Bowel Response against *Toxoplasma gondii*[1]

Catherine Ronet,* Sylvie Darche,* Maria Leite de Moraes,† Sachiko Miyake,‡ Takashi Yamamura,‡ Jacques A. Louis,* Lloyd H. Kasper,[2§] and Dominique Buzoni-Gatel[2,3]*

**We demonstrated in this study the critical role of NKT cells in the lethal ileitis induced in C57BL/6 mice after infection with *Toxoplasma gondii*. This intestinal inflammation is caused by overproduction of IFN-γ in the lamina propria. The implication of NKT cells was confirmed by the observation that NKT cell-deficient mice (Jα281$^{-/-}$) are more resistant than C57BL/6 mice to the development of lethal ileitis. Jα281$^{-/-}$ mice failed to overexpress IFN-γ in the intestine early after infection. This detrimental effect of NKT cells is blocked by treatment with α-galactosylceramide, which prevents death in C57BL/6, but not in Jα281$^{-/-}$, mice. This protective effect is characterized by a shift in cytokine production by NKT cells toward a Th2 profile and correlates with an increased number of mesenteric Foxp3 lymphocytes. Using chimeric mice in which only NKT cells are deficient in the IL-10 gene and mice treated with anti-CD25 mAb, we identified regulatory T cells as the source of the IL-10 required for manifestation of the protective effect of α-galactosylceramide treatment. Our results highlight the participation of NKT cells in the parasite clearance by shifting the cytokine profile toward a Th1 pattern and simultaneously to immunopathological manifestation when this Th1 immune response remains uncontrolled. *The Journal of Immunology*, 2005, 175: 899–908.**

Natural killer T cells represent a minor subset of T lymphocytes that share receptor structures with conventional T cells and NK cells (1, 2). Murine NKT cells express intermediate levels of a TCR using a semi-invariant Vα14-Jα281 TCR α-chain paired with Vβ8, -7, or -2 TCR·β-chain together with NK cell receptors (NKR-P1, Ly-49, and NK1.1 in C57BL/6 mice) (3, 4). These cells are located mainly in the liver, spleen, thymus, and bone marrow and recognize Ag in the context of the monomorphic CD1d Ag-presenting molecule (5, 6). CD1d and the invariant TCR α-chain are essential for the normal development of NKT cells (7). CD1 molecules present hydrophobic lipid Ags (8), and the marine sponge derived glycolipid, commonly referred to as α-galactosylceramide (α-GalCer),[4] was identified as a potent stimulatory factor for NKT cells (9).

A potential role of NKT cells in the regulation of immune responses has been hypothesized because of their capacity to rapidly release large amounts of IL-4 and IFN-γ upon activation (10). NKT cells play crucial roles in various immune responses, including antitumor, autoimmune, and antimicrobial immune responses (1, 11). Within hours of TCR engagement, CD1d-reactive T cells produce Th1 and/or Th2 cytokines (9, 11, 12) by a mechanism not yet identified that can influence other immune cells, such as conventional T (13–15), NK cells (16), and dendritic cells (DC) (17). NKT cell-derived Th1 cytokines (such as IFN-γ) are important in the initiation of the antitumor immune response, whereas NKT cell-derived Th2 cytokines (IL-4 and IL-10) are involved in down-regulation of the autoimmune response (18). When stimulated with α-GalCer, NKT cells exhibit the ability to proliferate and to produce both Th1 and Th2 cytokines (9, 19). However administration of α-GalCer at the time of priming of mice with Ag results in the generation of only Ag-specific Th2 cells. Thus, α-GalCer might be useful for modulating the immune response toward a Th2 phenotype (12).

Recent evidence suggests that NKT cells are important in the host/pathogen immune response, including cytotoxicity, Ab production, and regulation of Th1/Th2 differentiation. NKT cells have been shown to participate in the immune response to a range of different infectious agents, including *Listeria*, *Mycobacteria*, *Salmonella*, *Plasmodium*, viral hepatitis (20, 21), HIV (22), and even *Toxoplasma gondii* (23). *T. gondii* is an obligate intracellular parasite acquired by oral ingestion of tissue cysts containing either bradyzoites or sporozoites from contaminated soil. It has been observed that after oral infection with tissue cysts, the intestinal epithelial and lamina propria cells are invaded by the parasites. Parasite infection induces a strongly biased Th1 response in the gut that displays a dual effect. IFN-γ produced by the CD4 T cells from the lamina propria (24) limits parasite replication, conferring resistance in mice in certain inbred strains. However, in C57BL/6 (B6) mice, an overwhelming IFN-γ production leads to a lethal acute ileitis within 10 days after oral infection. This *Toxoplasma*-induced intestinal disease shares histological and immunological similarities with human inflammatory bowel disease, such as

*Department of Parasitology, Unit of Early Responses to Intracellular Parasites and Immunopathology, Institut Pasteur-Institut National de la Recherche Agronomique, Paris, France; †Centre National de la Recherche Scientifique, Unité Mixte de Recherche, University René Descartes, Paris V, Hôpital Necker, Paris, France; ‡Department of Immunology, National Institute of Neuroscience, National Center of Neurology and Psychiatry, Tokyo, Japan; and §Departments of Medicine and Microbiology/Immunology, Dartmouth Medial School, Lebanon, NH 03756

Received for publication December 21, 2004. Accepted for publication May 7, 2005.

The costs of publication of this article were defrayed in part by the payment of page charges. This article must therefore be hereby marked *advertisement* in accordance with 18 U.S.C. Section 1734 solely to indicate this fact.

[1] C.R. was the recipient of fellowships from the Association Francois Aupetit and the Joshui/Institut Pasteur Foundation. This work was carried out in the Unit of Early Responses to Intracellular Parasites and Immunopathology and was supported by the Pasteur Institute, the Institut National de la Recherche Agronomique, the Fondation pour la Recherche Médicale. Partial support for this work was provided by National Institutes of Health Grant AI19613.

[2] L.H.K. and D.B.-G. share senior authorship.

[3] Address correspondence and reprint requests to Dr. Dominique Buzoni-Gatel, Department of Parasitology, Unit of Early Responses to Intracellular Parasites and Immunopathology, Institut Pasteur-Institut National de la Recherche Agronomique, 25 rue du Dr Roux, 75724 Paris Cedex 15, France. E-mail address: buzoni@pasteur.fr

[4] Abbreviations used in this paper: α-GalCer, α-galactosylceramide; DC, dendritic cell; IEL, intraepithelial lymphocyte; LPL, lamina propria lymphocyte; MLN, mesenteric lymph node; SAG1, surface Ag-1.



0022-1767/05/$02.00

Crohn's disease. The regulation of this inflammatory process requires a delicate homeostatic balance that is influenced by either a Th1 or Th2 response.

In this report the role of NKT cells in the initiation of the inflammatory process in response to oral infection with *T. gondii* was evaluated. Our findings suggest a potentially critical role for these early responder cells in the initiation and regulation of the lethal inflammatory process.

## Materials and Methods

### *Mice and parasites*

Female, 8- to 10-wk-old, inbred B6 mice and CBA were obtained from IFFA-Credo. Mice were housed under approved conditions of the Animal Research Facility at Institut Pasteur. IL-$10^{-/-}$ mice were supplied by Dr. Bandeira (Institut Pasteur, Paris, France). We were provided with J$\alpha$281$^{-/-}$ mice by Dr. M. Taniguchi (Riken Research Center for Allergy and Immunology, Yokohama, Japan) (9), V$\alpha$14Tg mice by Dr. A. Lehuen (Institut National de la Santé et de la Recherche Médicale, Paris, France) (25), actin-GFP mice by Dr. M. Okabe (Genome Information Research Center, Osaka University, Osaka, Japan) (26), and CD1$^{-/-}$ mice by Dr. L. Van Kaer (Vanderbilt University School of Medicine, Nashville, TN) (7). All the genetically modified strains were on a B6 genetic background. 76K strain cysts isolated from the brains of chronically infected CBA mice were used for in vivo studies. Mice were infected orally by intragastric gavage of 35 cysts, a lethal condition for B6 wild-type mice as described previously (27). After infection, mortality was evaluated, and morbidity was estimated by the percentage of weight loss compared with the initial weight.

### *Treatment with α-GalCer, anti-CD25, or anti IL-4 Abs*

α-GalCer was kept dissolved in PBS buffer containing 20% DMSO at 220 μg/ml as a stock solution. Mice received a single i.p. injection of 5 mg of α-GalCer the day before infection by *T. gondii*. Control mice received an i.p. injection of PBS/20% DMSO, which has no influence on the course of *T. gondii* infection.

Neutralization of IL-4 was conducted by injecting i.p. 1 mg of anti-IL-4 (11B11; provided by Dr. P. Launois, World Health Organization Immunology Research and Training Center, Institute of Biochemistry, Epalinges, Switzerland) mAb 24 h before α-GalCer treatment and 48 h before infection. Control mice were treated with rat IgG Abs (Sigma-Aldrich).

Mice were depleted of CD25$^+$ cells by i.p. administration of 0.5 mg of anti-CD25 (PC61; provided by Dr. R. J. Noelle, Dartmouth Medical School, Lebanon, NH) mAb. Three days after the treatment, the efficiency of CD25$^+$ cell depletion was controlled in peripheral blood by FACS analysis. The CD25$^+$ cell depletion remained stable over 15 days. Control mice were treated with a mouse IgD1 isotype Ab (MOPC31C k; BD Pharmingen).

### *Cell purification*

***Lamina propria.*** The method used to isolate intestinal lamina propria lymphocytes (LPLs) was modified as described previously (24). After dissection and removal of Peyer's patches, the sectioned intestines were incubated in PBS-3 mM EDTA at 37°C and 5% $CO_2$ (four times, 20 min each time). Then intestinal pieces were incubated at 37°C in RPMI 1640-5% FCS with Liberase (0.14 Wunch units/ml; Roche) and DNase (10 U/ml; Sigma-Aldrich). After 45 min, the digested suspension containing LPLs was filtered on a cell strainer and washed twice, and the pellet was submitted to a Percoll gradient to isolate the lymphocytes. Total cells were resuspended in a 80% isotonic Percoll solution (Pharmacia Biotech) and overlaid with a 40% isotonic Percoll solution. Centrifugation for 30 min at 3000 rpm resulted in concentration of mononuclear cells at the 40–80% interface. The collected cells were washed once with PBS supplemented with 2% FCS. The purity of the LPL population was assessed by the relative percentage of B cells (>50%), CD4 T cells (~20%), CD8 T (<3%) cells, and enterocytes (<5%).

***Intraepithelial lymphocytes (IELs).*** IELs were isolated as previously described (28). Briefly, the small intestine was flushed with PBS and divided longitudinally after removal of Peyers's patches. The mucosae were scraped, dissociated by mechanical disruption, in RPMI 1640 containing 4% FCS and 1 mmol/L DTT. After passage over a glass-wool column, the lymphocytes were separated by Percoll as described for LPLs. The purity of IEL population was assessed by the relative percentages of B cells (<2%), CD4 T cells (<10%), CD8 T cells (>80%), and enterocytes (<5%).

***Mesenteric lymph node (MLN) and spleen.*** MLN and spleen were dissociated and freed of connective tissue by filtration (70 μm). Unless otherwise stated, each mouse was analyzed individually.

***Liver.*** Single-cell suspensions were obtained from liver as described previously by us (29).

### *Cytometric analysis*

***FACS analysis of NKT cells.*** Single-cell suspensions were first incubated 10 min with an anti-FcγRII/III mAb (Fcblock, 2.4G2; BD Pharmingen), followed by a 1-h exposure to CD1d/α-GalCer tetramer-allophycocyanin under agitation at 4°C. CD1d/α-GalCer tetramers were prepared as described by Matsuda et al. (30). After two washes, other cell surface stainings were performed with the following Abs: anti-TCRβ (H57-597), anti-CD4 (RM4-5), anti-CD8 (53-6.7), anti-NK1.1 (PK136), anti-CD25 (C363 16A), anti-CD45RB (7D4), and anti-CD5 (BD Biosciences). PerCP-streptavidin and CyChrome-streptavidin were purchased from BD Biosciences. Cells were analyzed in PBS containing 2% FCS using a FACSCalibur flow cytometer and CellQuest software (BD Biosciences).

***Cell sorting.*** NKT cells stained with the tetramer were magnetically sorted. After tetramer CD1d/α-GalCer-allophycocyanin staining, cells suspensions were incubated for 15 min in PBS/2% FCS/2 mM EDTA at 4°C with anti-allophycocyanin beads as described by the provider (Miltenyi Biotec). After washing and filtration, samples were run on AutoMACS (Miltenyi Biotec). Purity was controlled by cytometric analysis, and the sorted cells were frozen until molecular biology analysis.

For the reconstitution experiment, NKT from the liver and the spleen of actin-GFP mice were sorted with both anti-CD5 biotin (53-7.3), and anti-NK1.1-PE (PK136) mAbs and streptavidin-allophycocyanin using a MoFlo (DakoCytomation). Purified NKT-GFP$^+$ cells were collected in RPMI 1640 supplemented with 10% FCS. The purity of the sorted NKT-GFP cells was found to exceed 97%.

***Adoptive transfer of NKT-GFP$^+$ cells.*** Highly purified NKT cells ($1 \times 10^6$) were injected i.v. into J$\alpha$281$^{-/-}$ mice. At the same time these mice were treated with 5 μg of α-GalCer i.p. One day later, NKT cells were transferred, and α-GalCer-treated mice were infected.

### *Histological examination*

***Histopathology and morphometric analysis.*** Intestines were immediately fixed in buffered 10% formalin after dissection. Then they were embedded, sectioned, and stained with H&E for histological examination. Inflammation was scored by the ratio of the length/thickness of the villi (mean of 20 measures for a total of four different fields).

***Confocal microscopic examination.*** Intestinal and hepatic samples from NKT-GFP-transferred mice were microscopically examined. On day 7 after infection mice were scarified, and samples from intestines and livers were incubated for 24 h in paraformaldehyde (4%) and saccharose (30%). Then tissues were frozen in liquid nitrogen using OCT embedding compound (Sakura). Frozen sections (10 μm) were cut on a microtome HM 505 cryostat (Microcom Laboratory), fixed with PBS/paraformaldehyde (4%), permeabilized by PBS/Triton (0.1%), contrastained with rhodamine phallodin (Molecular Probes), and mounted with Vectashield (Vector Laboratories). Preparations were analyzed with fluorescent microscope Axioplan 2 imaging coupled with an ApoTome system (Zeiss). GFP-NKT cell trafficking was also assessed by FACS analysis performed on day 7 after infection with cell suspensions obtained from lamina propria and livers.

### *Bone marrow chimeric mice*

Recipient mice were lethally irradiated (900 rad) with a $^{137}$Ce source. Then they received i.v. bone marrow cells ($1 \times 10^7$) recovered from femurs and tibias of donor mice. To generate mice with only NKT cells devoid of the IL-10 gene, a mix (50/50%) of bone marrow cells from J$\alpha$281$^{-/-}$ mice and IL-$10^{-/-}$ mice was prepared. Control mice received cells from B6, J$\alpha$281$^{-/-}$ or IL-$10^{-/-}$ mice alone. Six weeks after reconstitution, mice were bled, and the presence of CD4$^+$, CD19$^+$ (1D3), and CD11c$^+$ (HL3) cells was monitored by flow cytometric analysis. Reconstitution with NKT was assessed (two mice per group) by staining the CD1d/α-GalCer-allophycocyanin tetramer cell suspensions obtained from the liver and lamina propria of the chimera. Chimeric mice were then infected. At different times after infection, LPLs and MLN cell suspensions were phenotyped by FACS analysis. Morbidity was evaluated daily by recording the weight loss, and mortality was also recorded.

### *RNA extraction, cDNA preparation, and real-time RT-PCR*

Tissue samples from intestines and purified cells were kept frozen (−70°C) until mRNA extraction. Specimens were disrupted in a Polytron (Brinkmann Instruments) and homogenized in 350 ml of RLT buffer (Qiagen).

RNA extraction and cDNA preparation were conducted following standard procedures using oligo(dT)$_{17}$ primers, and 10 U of avian myeloblastosis virus reverse transcriptase. Quantitative PCR was performed with the GeneAmp 7000 (Applied Biosystems) as indicated by the supplier. Primers and probes for the quantitative PCR assay of cytokines and actin were designed as previously described (31). Foxp3 mRNA were analyzed with applied assay on demand n°Mm00475156_m1 (Applied Biosystems).

### *Parasite burden*

DNA was extracted from the different organ samples using a DNAeasy kit (Qiagen). The *Toxoplasma* B1 gene was amplified by quantitative real-time PCR (32). Parasite titration by real-time PCR was performed with the GeneAmp 7000 (Applied Biosystems). The standard curve established from the serial 10-fold dilutions of *T. gondii* DNA of parasite concentrations ranging from $1 \times 10^6$ to 10, showed linearity over a 6-log concentration range and was included in each amplification run. At different time points after infection, tissue samples were recovered, and their DNA were extracted with the DNeasy Tissue Kit (Qiagen). For each sample, parasite count was calculated by interpolation from the standard curve. The parasite burden was expressed as the number of parasites per milligram of samples. Cerebral parasite burden was evaluated by enumeration of the cysts on day 30 after infection.

### *Statistical analysis*

Results are expressed as the mean ± SD. Statistical differences between groups were analyzed using Student's *t* test. A value of $p < 0.05$ was considered significant.

## Results

### *Presence of NKT cell in the lamina propria*

The presence of the NKT lymphocyte subpopulation within the gut was demonstrated by FACS analysis using the CD1d/α-GalCer tetramers. In the lamina propria of naive B6 mice, 2% of the mononuclear cells (LPLs) were detected (Fig. 1*A*). NKT cells were not detected in cell suspensions from the IEL compartment (Fig. 1*A*). Seventy to 80% of the tetramer-positive cells were CD4$^+$; the remainder were CD4$^-$CD8$^-$ double negative. During the days following infection, a decrease in the number of tetramer-positive cells was observed (Fig. 1*B*) that could be due to TCR down-regulation. Serial time point phenotyping after infection demonstrated that all NKT cells were CD25$^-$. To assess NKT cell trafficking into the intestine after infection, Jα281$^{-/-}$ mice were transferred with NKT-GFP$^+$ cells ($1 \times 10^6$) highly purified from the livers of GFP transgenic mice on the basis of CD5 and NK1.1 expression (Fig. 1*D*, *a*). At 7 days after infection, GFP$^+$ cells were found in cell suspension obtained from the liver (Fig. 1*D*, *b*) and lamina propria (Fig. 1*D*, *c*) of the transferred mice. Histological examination by confocal microscopy revealed that within the liver, NKT-GFP$^+$ cells were distributed among hepatocytes near the sinusoids (Fig. 1*E*). Within the gut, NKT-GFP$^+$ cells were always

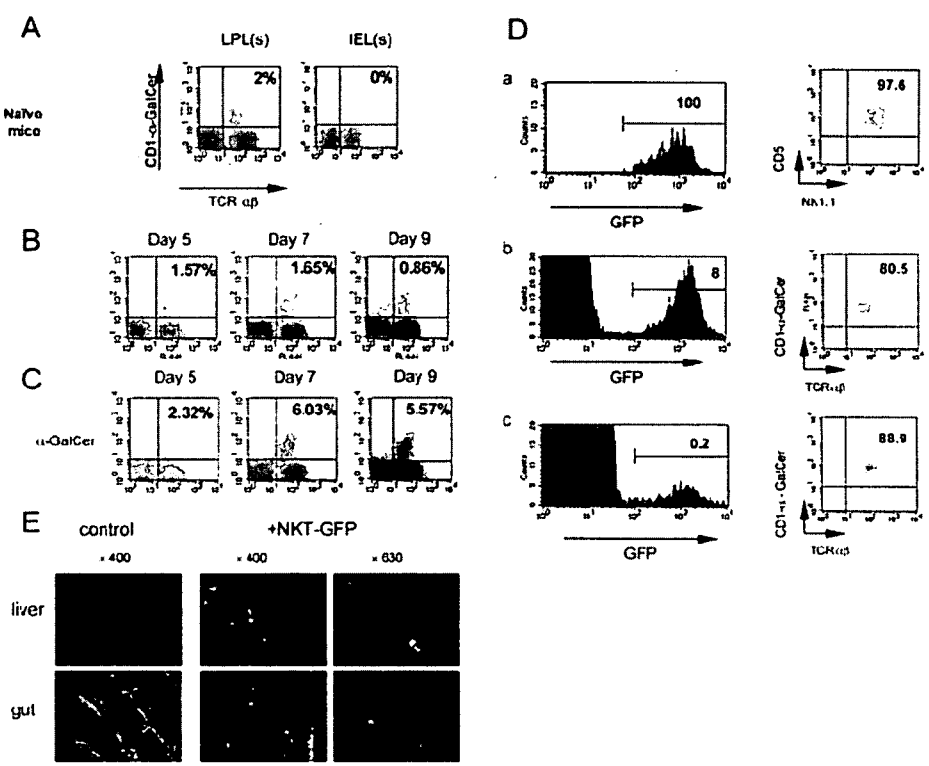


FIGURE 1. NKT cells are present in the lamina propria compartment. *A*, Representative FACS profiles showing Vα14 CD1d/α-GalCer$^+$TCRαβ$^-$ cells obtained from LPL and IEL suspension from naive mice. The numbers indicate the proportion of tetramer-positive T cells in the lymphocyte gate. This analysis was performed with five mice and was repeated twice. *B*, Representative FACS profiles showing Vα14 CD1d/α-GalCer$^+$TCRαβ$^+$ cells obtained from LPL suspensions of mice at different times after infection. This analysis was performed with five mice individually and was repeated twice. *C*, Representative FACS profiles showing Vα14 CD1d/α-GalCer$^+$TCRαβ$^+$ cells obtained from LPL suspensions of α-GalCer-treated mice at different times after infection. This analysis was performed with five mice and was repeated twice. *D*, NKT cell populations from actin-GFP mice were purified on the basis of GFP, CD5, and NK1.1 (PE) expression and were positively selected with magnetic beads directed against PE. *D*, *a*, Purity of the selected NKT cell population. One million purified NKT cells were injected i.v. into Jα281$^{-/-}$ mice. The following day, these mice were infected with *T. gondii*. On day 7 after the adoptive transfer, Jα281$^{-/-}$ recipients showed a significant presence of GFP$^+$ cells in the liver (*b*) and lamina propria (*c*) cell suspension, which are almost all NKT cells as revealed by CD1d/α-GalCer$^+$ staining after gating on GFP$^+$ cells. Four mice were adoptively transferred with NKT-GFP cells, requiring 24 GFP transgenic donor mice. *E*, GFP$^+$ NKT cells were detected in paraformaldehyde-fixed cryosections of liver and intestine from Jα281$^{-/-}$ recipient mice (the control was sections from naive Jα281$^{-/-}$mice). Actin filaments were stained in red with rhodamine phallodin to visualize the organ structure. Original magnifications: ×400 and ×630. The pictures shown are representative of observations made with the four NKT-GFP cell recipient mice.

localized in the lamina propria and were never associated with the IEL compartment (Fig. 1*E*). These data indicated that NKT cells traffic to the intestine, where they localize within the lamina propria.

### *Importance of NKT cells in the development of acute inflammatory ileitis in B6 mice*

The involvement of NKT cells in the initiation of the intestinal inflammation after oral infection with *T. gondii* was investigated by comparing the outcome of the infection in wild-type B6 mice and mice genetically deficient in NKT cells ($J\alpha281^{-/-}$ mice). As expected, all control B6 mice died within 7–10 days of severe ileitis after oral challenge with 35 cysts (Fig. 2*A*). The intestinal inflammation and subsequent morphological changes were characterized by cellular infiltration within the lamina propria; short, thickened villi; and patchy transluminal necrosis. In contrast, $J\alpha281^{-/-}$ mice developed a less severe disease (Fig. 2*B*) associated with 1) a decrease in the length/thickness ratio of the villi compared with B6 infected mice (Fig. 2*C*), 2) a significantly delayed time of death, and 3) a decrease in the mortality rate compared with B6 mice (Fig. 2*A*). This outcome was not parasite dose dependent, as determined using a lower infectious dose of cysts (10 cysts/mouse) in which all the $J\alpha281^{-/-}$ mice survived, whereas 25% of the B6 died (Fig. 2*D*). These results indicate that the absence of NKT cells correlates with a more resistant phenotype. However, $CD1d^{-/-}$ mice were even more susceptible than B6 mice (Fig. 2*A*). In addition to NKT depletion, regulatory cells, such as IEL and B cells, are also reduced in $CD1d^{-/-}$ mice (33, 34).

To further explore the potential role of NKT cells in the inflammatory process, mice that overexpressed NKT cells (Vα14Tg mice) were infected. Both B6 and Vα14Tg mice died within 7–10 days when infected with 35 cysts (Fig. 2*A*). However, in the experiment using a lower dose of cysts (10 cysts/mouse), all the Vα14Tg mice died, whereas only 25% of the B6 mice died (Fig. 2*D*). These data confirm that NKT cells are important in the innate host response to oral parasite infection and are involved in disease susceptibility.

### *NKT cell activation correlates with intestinal IFN-γ production after* T. gondii *infection*

IFN-γ is an important cytokine in mediating host defense against *T. gondii* infection. It limits parasite replication, but, at the same time, if overproduced, it leads to the development of overwhelming intestinal inflammation. Therefore, because NKT cell-deficient

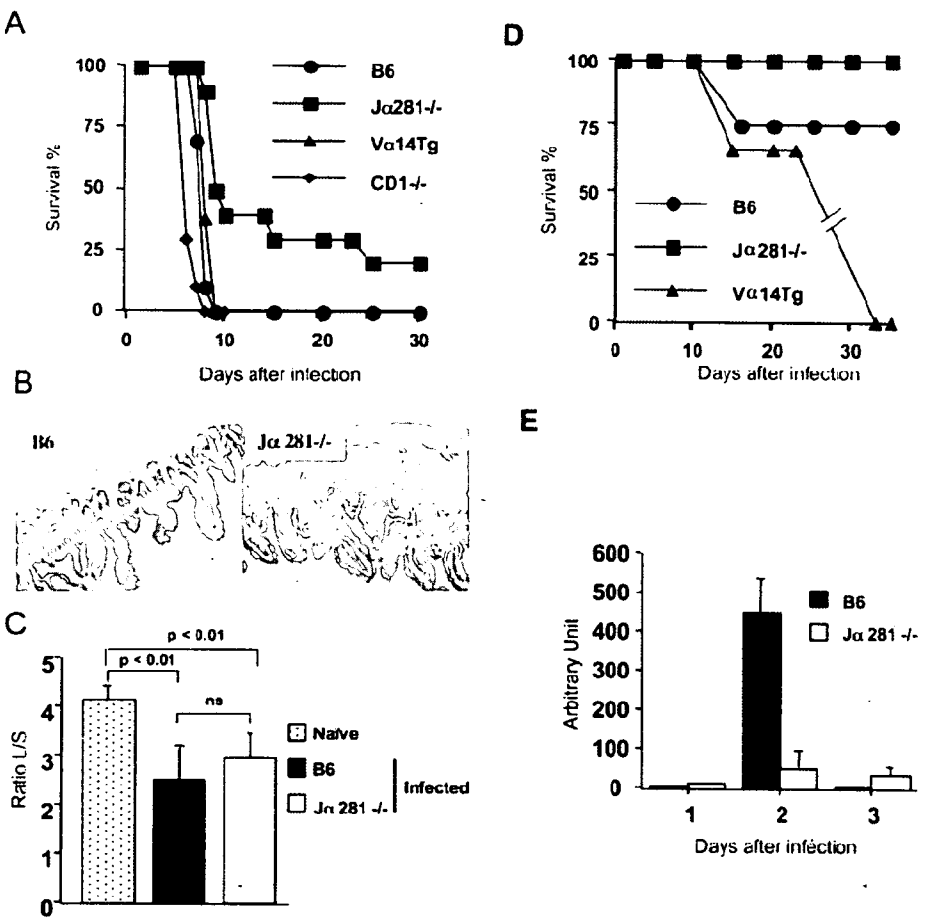


FIGURE 2. NKT cells are involved in the development of acute inflammatory ileitis in B6 mice. *A*, Survival rate of B6, $J\alpha281^{-/-}$, Vα14Tg, and $CD1d^{-/-}$ mice after challenge with 35 cysts of *T. gondii* ($n$ = 10/group). Data are representative of three independent experiments with similar results. *B*, Intestinal H&E histology from B6 and $J\alpha281^{-/-}$ mice on day 7 after challenge (magnification, ×200). Results are representative of two independent experiments performed with four mice each time. *C*, Intestinal lesions from B6 and $J\alpha281^{-/-}$ on day 7 after challenge were scored as the ratio of the villi length to its thickness. These data were the mean of 20 measures obtained with four different fields and repeated with two mice per group. *D*, Survival rate of B6, $J\alpha281^{-/-}$, Vα14Tg after challenge with 10 cysts of *T. gondii* ($n$ = 5/group). Data are representative of two independent experiments with similar results. *E*, Early IFN-γ mRNA expression in the intestine after infection is dependant upon the presence of NKT cells. Samples from the ileum of B6 and $J\alpha281^{-/-}$ mice were analyzed for mRNA expression of IFN-γ by real-time RT-PCR. Results are expressed as the fold increase relative to noninfected control mice after normalization with the housekeeping gene. The mean ± SD were calculated from two samples from two mice. Results are representative of three independent experiments.

mice (Jα281$^{-/-}$) were more resistant to the development of lethal ileitis after *T. gondii* infection, the expression of IFN-γ in their intestines was measured at different times after oral challenge with the cysts. Between days 2 and 3 after infection, IFN-γ mRNA expression peaked in the intestine of B6 mice, and there was a significant difference in IFN-γ mRNA expression between B6 mice and Jα281$^{-/-}$ mice. By quantitative RT-PCR, the level of mRNA expression in B6 mice was 9–10 times higher than that in Jα281$^{-/-}$ mice (Fig. 2*E*). Over time, inflammatory cytokine production in Jα281$^{-/-}$ mice may increase, contributing in the delayed time to death due to lethal intestinal inflammation. The lack of early production of IFN-γ might also explain the 2-fold increase in parasite burden in Jα281$^{-/-}$ mice on day 8 after infection. These findings strongly suggest that NKT cell activation after oral infection with *T. gondii* is associated with early initiation of the Th1 process observed in the intestines of B6 mice.

*Treatment with α-GalCer protects against the development of lethal ileitis*

Because α-GalCer can influence the nature of the cytokines produced by NKT cells and consequently the orientation of the adaptative Th response, mice were treated with α-GalCer the day before infection. Up to 30 days after infection, this treatment prevented death in both B6 (100%) and Vα14Tg mice overexpressing NKT cells (80%; Fig. 3*A*). Histological examination performed on day 7 after infection revealed that treatment with α-GalCer interfered with the development of ileitis (Fig. 3, *B* and *C*). In addition, B6 mice treated with α-GalCer exhibited less weight loss compared with untreated infected controls (Fig. 3*D*). To assess the cell population targeted by α-GalCer treatment, NKT-deficient mice (Jα281$^{-/-}$) were treated with α-GalCer the day before infection. This treatment had no effect on the infection outcome in Jα281$^{-/-}$ mice (Fig. 3*A*), as attested by the early time of death and the histological damages observed in treated mice (Fig. 3*B*). These observations strongly suggest that α-GalCer modulates the functional abilities of NKT cells. Treatment with α-GalCer was not directly toxic to the parasite, because there was no difference in parasite burden in Jα281$^{-/-}$ mice treated or not treated on day 30 after infection (data not shown). Treatment with α-GalCer 2 days after infection failed to impact the development of the hyperinflammatory response in small intestine.

*Treatment with α-GalCer induces preferential production of IL-4 and IL-10 in* T. gondii*-infected mice*

One of the consequences of α-GalCer treatment was the increase in the number of NKT cells in the lamina propria of infected mice (Fig. 1*C*). The production of selected cytokines in the whole intestine of α-GalCer-treated mice was monitored by quantitative RT-PCR. A significant increase in IL-10 (180-fold) and IL-4 (80-fold) mRNA expression was observed in the intestines of α-GalCer-treated mice on days 3 and 5, respectively, after infection. In contrast, no increase in IL-13 mRNA expression in the whole intestine of α-GalCer-treated mice was measured at serial time points after infection. mRNA for IFN-γ was also significantly decreased (10-fold) in α-GalCer-treated mice (data not shown). This result demonstrated a shift in cytokine production toward a Th2-like profile after treatment with α-GalCer and infection and a decline in the Th1-like immune response. To better assess the contribution of intestinal NKT cells in this shift, α-GalCer-treated mice and untreated control mice were killed on day 8 after infection, and NKT cells were purified from the lamina propria (Fig. 4*A*). As shown in Fig. 4*A*, the purity of the sorted population was

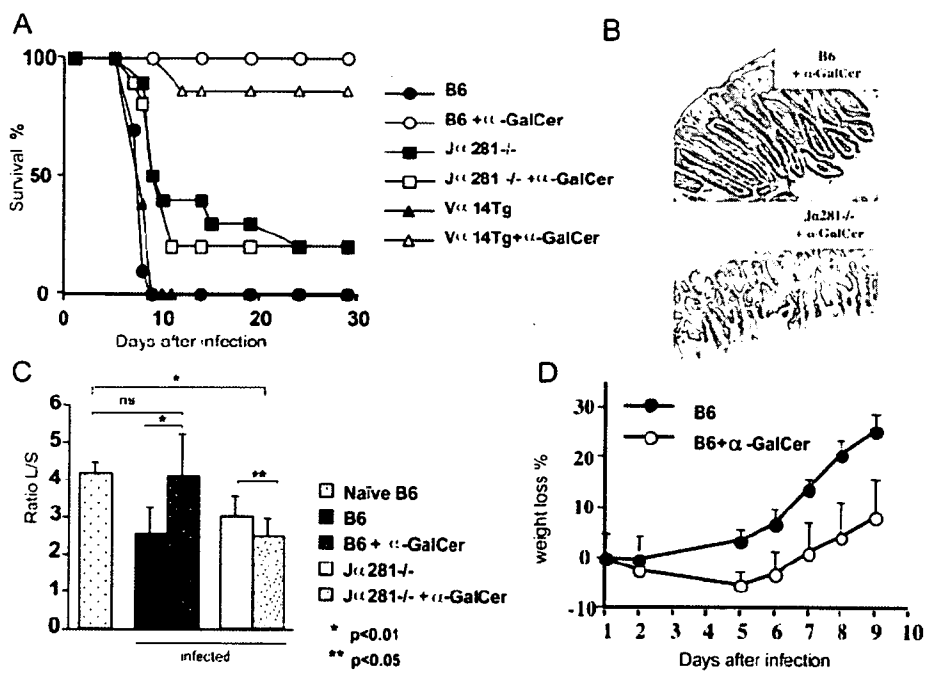


FIGURE 3. α-GalCer treatment protects the infected mice against the development of lethal ileitis. *A*, Survival rates of B6, Jα281$^{-/-}$, and Vα14Tg mice after i.p. administration of 5 μg of α-GalCer the day before challenge with *T. gondii* ($n$ = 10/group). Results are representative of two independent experiments. *B*, Intestinal H&E histology of α-GalCer-treated or untreated mice on day 7 after infection (magnification, ×200). *C*, Intestinal lesions in α-GalCer-treated or untreated mice on day 7 after infection were scored as the ratio of the villi length to its thickness. These data were the mean of 20 measures obtained with four different fields and repeated with two mice per group. *D*, B6 mice treated with α-GalCer exhibited only mild weight loss compared with untreated infected controls. Infected B6 mice treated, or not, with α-GalCer were weighed daily. Weight loss is expressed as a percentage of the animal's initial weight.